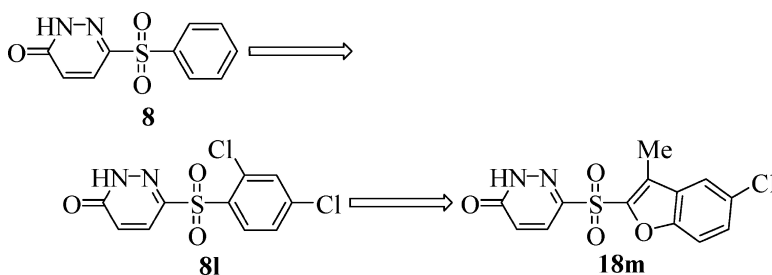


## A Novel Series of Non-Carboxylic Acid, Non-Hydantoin Inhibitors of Aldose Reductase with Potent Oral Activity in Diabetic Rat Models: 6-(5-Chloro-3-methylbenzofuran-2-sulfonyl)-2H-pyridazin-3-one and Congeners

Banavara L. Mylari, Sandra J. Armento, David A. Beebe, Edward L. Conn, James B. Coutcher, Michael S. Dina, Melissa T. O'Gorman, Michael C. Linhares, William H. Martin, Peter J. Oates, David A. Tess, Gregory J. Withbroe, and William J. Zembrowski  
*J. Med. Chem.*, **2005**, 48 (20), 6326-6339 • DOI: 10.1021/jm050462t • Publication Date (Web): 10 September 2005

Downloaded from <http://pubs.acs.org> on March 28, 2009



### More About This Article

Additional resources and features associated with this article are available within the HTML version:

- Supporting Information
- Links to the 3 articles that cite this article, as of the time of this article download
- Access to high resolution figures
- Links to articles and content related to this article
- Copyright permission to reproduce figures and/or text from this article

[View the Full Text HTML](#)

# A Novel Series of Non-Carboxylic Acid, Non-Hydantoin Inhibitors of Aldose Reductase with Potent Oral Activity in Diabetic Rat Models: 6-(5-Chloro-3-methylbenzofuran-2-sulfonyl)-2H-pyridazin-3-one and Congeners

Banavara L. Mylari,\* Sandra J. Armento, David A. Beebe, Edward L. Conn, James B. Coutcher, Michael S. Dina, Melissa T. O’Gorman, Michael C. Linhares, William H. Martin, Peter J. Oates, David A. Tess, Gregory J. Withbroe, and William J. Zembrowski

Pfizer Global Research and Development, Pfizer Inc., Groton, Connecticut 06340

Received May 16, 2005

Discovery of a highly selective, potent, and safe non-carboxylic acid, non-hydantoin inhibitor of aldose reductase (AR) capable of potently blocking the excess glucose flux through the polyol pathway that prevails under diabetic conditions has been a long-standing challenge. In response, we did high-throughput screening of our internal libraries of compounds and identified 6-phenylsulfonylpyridazin-2H-3-one, **8**, which showed modest inhibition of AR, both in vitro and in vivo. Initial structure–activity relationships concentrated on phenyl substituents and led to 6-(2,4-dichlorophenylsulfonyl)-2H-pyridazin-3-one, **8l**, which was more potent than **8**, both in vitro and in vivo. Incorporation of extant literature findings with other aldose reductase inhibitors, including zopolrestat, resulted in the title inhibitor, **19m**, which is one of the most potent and highly selective non-carboxylic acid, non-hydantoin inhibitors of AR yet described (IC<sub>50</sub>, 1 nM; ED<sub>90</sub> vs sciatic nerve sorbitol and fructose, respectively, 0.8 and 4.0 mg/kg). In rats, its oral bioavailability is 98% and it has a favorable plasma *t*<sub>1/2</sub> (26 ± 3 h).

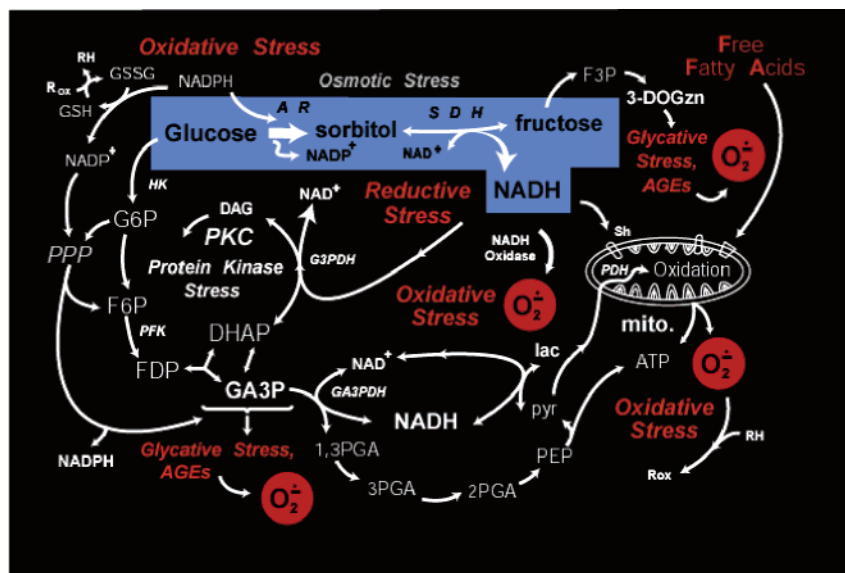
## Introduction

Diabetes mellitus has become pandemic and according to reports, including a forecast by the World Health Organizations, there will be a sharp increase in the total number of cases worldwide by 2030, especially in the two most populous countries, China and India.<sup>1</sup> In fact, India could be bracing itself for the dubious distinction of becoming the diabetes capital of the world. This is an ominous forecast, because managing the long-term complications of the disease, which include nephropathy, neuropathy, retinopathy, and cardiovascular complications, will have a serious impact on public health budgets. For example, an American Diabetes Association estimate puts the total costs for diabetes care in the United States in 2002 at \$132 billion. Direct medical expenditures alone totaled \$91.8 billion, of which \$24.6 billion accounted for chronic complications attributable to diabetes.<sup>2</sup> These include hospital and in-patient care to provide for limb amputation (a complication of serious neuropathy), cataract surgery, retinal coagulation therapy, and kidney dialysis. Results of the Diabetes Control and Complications Trial (DCCT)<sup>3</sup> and the United Kingdom Perspective Diabetes Study (UK PDS)<sup>4</sup> have underscored the link between chronically elevated blood glucose levels and the severity of the consequent diabetic complications as well as the critical importance of controlling and maintaining near normal blood glucose excursions. While the exact mechanism(s) underlying the pathological consequences of chronically high blood glucose levels is not yet fully understood, considerable attention has focused on one aspect of metabolic research that pertains to the primary consequences of

high intracellular glucose flux through the polyol pathway<sup>5,6</sup> (Figure 1, shaded in blue), viz., cellular osmotic stress<sup>7</sup> and pseudohypoxia-linked oxidative stress.<sup>8</sup>

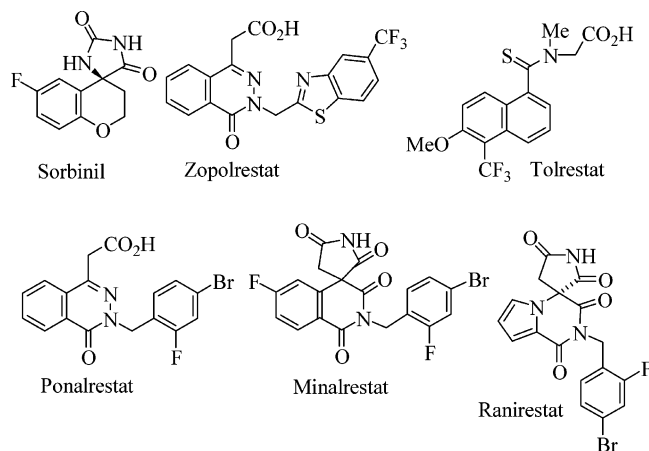
Figure 1 also calls attention to several other downstream events tied to the polyol pathway, for example, protein kinase stress and glycation stress. From a potential successful therapeutic approach, a robust blockade of excess glucose flux through both steps of the polyol pathway, with a powerfully effective aldose reductase inhibitor (ARI), to completely normalize both cellular sorbitol and fructose pools, would not only address the osmotic and the oxidative stress hypotheses but also the other downstream markers. It is noteworthy that, in the streptozotocin diabetic rat model, suppression of nerve fructose lags behind that of sorbitol by a factor of 3–20-fold, confirming that just inhibition of sorbitol is not a satisfactory marker for robust control of glucose flux through the polyol pathway.<sup>6d</sup> Animal data with sorbitol dehydrogenase inhibitors further confirms that flux through the polyol pathway is quite active, even in the nondiabetic state, e.g., in normal rats.<sup>9</sup> In other words, near normalization of fructose levels requires near overnormalization of sorbitol levels. Strong support for this notion derives from dose titration using different ARIs, aimed at studying relationships between polyol pathway metabolites and tissue function. For example, a nearly full correction of the nerve conduction velocity deficit (NCV) in diabetic rats requires doses of ARIs that not only overnormalize nerve sorbitol levels but also suppress nerve fructose levels ≥90%.<sup>10,11</sup> In retrospect, clinical dose selection for all ARIs, including tolrestat, Ponalrestat, zopolrestat, and sorbinil (Chart 1), which were taken into placebo controlled phase III neuropathy studies in the United States and Europe, was based exclusively on safety and

\* To whom correspondence should be addressed. Phone: (860) 691-2033. Fax: (860) 739-7450. E-mail: blmylari@aol.com.



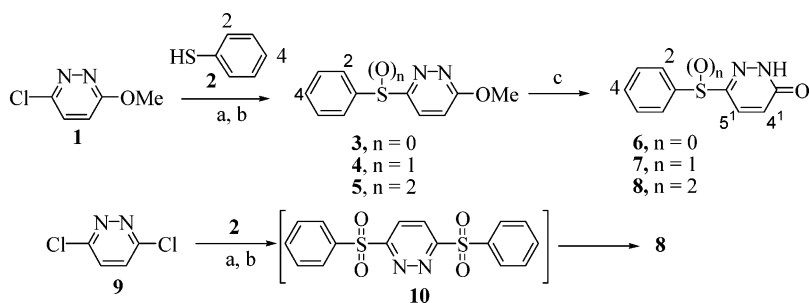
**Figure 1.** Polyol pathway network.

### Chart 1

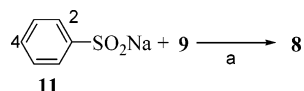


sorbitol suppression end point in diabetic rat models. In fact, none of the inhibitors has been shown to effect robust suppression of fructose in human tissues, for example, sural nerve biopsy samples, in a placebo-controlled large-scale efficacy trial. Furthermore, these ARIs were either carboxylic acids or spirohydantoin (broadly referred to as spiroimides). The major shortcoming of carboxylic acids is their poor tissue penetration, inherent to the conspicuous difference between their  $pK_a$ s (between 3 and 4) and blood pH (~7.4), resulting in poor distribution from blood to the tissues, and that of hydantoin-like spiroimides is the phenytoin-like hypersensitivity safety issue, both of which are well documented.<sup>12</sup> In view of the clinical dose selection issue and the dearth of new ARI chemotypes, perhaps it is not too surprising that no inhibitor has reached the market broadly yet. While the potential of ARIs in complications of cardio-renal tissues has long been recognized,<sup>13,14</sup> so far only feeble attempts have been made in clinical follow up. Major preoccupation on neuropathy may have detracted attention away from investigating clinical potential of ARIs in nephropathy and cardiac abnormalities. The positive effects seen in animal models with ARIs in the kidney<sup>13</sup> and the heart<sup>14</sup> warrant more focused and dedicated future follow up clinical investigations.

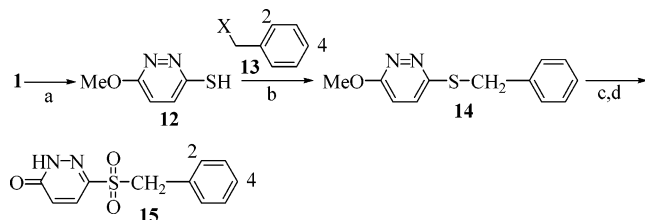
Because there is as yet no safe and effective ARI therapy available worldwide, the question has been raised whether the polyol approach to diabetic complications merits continued medicinal chemistry attention and whether one can discover an ARI of distinct chemical structure with sufficient potency and duration of action to effectively block the excess flux at safe doses in the clinic. We believe there are several compelling new findings to justify continued diligence and optimism. (1) Strong support comes from results of AR knockout mouse studies<sup>15</sup> and from reports that several allelic variants of the human AR gene that are associated with overexpression of AR are also associated with a significant increase in the risk of development of microvascular complications.<sup>16</sup> (2) Exciting clinical results have been obtained with the spiroimide ARI ranirestat (AS-3201),<sup>17</sup> in a just completed placebo-controlled 12-week study, in diabetic neuropathic patients. Ranirestat is reported to penetrate the human sural nerve sufficiently well to inhibit both sorbitol and fructose accumulation and, concomitantly, markedly improve nerve function as well as clinical measures of neuropathy in a dose-dependent manner.<sup>18</sup> (3) Also, there is an extremely encouraging earlier report that minalrestat, another spiroimide, in an open label, short-term clinical study strongly suppressed both sorbitol and fructose in sural nerve biopsy samples, as well as improved NCV, at very low doses.<sup>19</sup> (4) For the first time with any ARI, encouraging positive results have been obtained with zopolrestat in a placebo-controlled, double-blind clinical trial aimed at treating cardiac abnormalities in diabetic patients with neuropathy, particularly under an exercise regimen.<sup>20</sup> These contemporary findings have lent strong timely support for an initiative that we undertook some years ago to discover a novel chemical class of ARIs with potency clearly superior to both sorbinil and zopolrestat. In a previous publication in this journal,<sup>21</sup> we have given a preliminary account of a highly selective, orally potent non-carboxylic acid, non-hydantoin inhibitor of AR that normalized elevated levels of both sorbitol and fructose in the sciatic nerve of chronically diabetic rats at very low doses. Herein, we present the details of that account, including SAR

Scheme 1<sup>a</sup>

<sup>a</sup> Reagents and conditions: (a) Na/MeOH, PhMe or  $\text{KHCO}_3/\text{Ac}_2\text{O}$  or  $\text{KOt-Bu}/\text{DMF}$ . (b) MCPBA/ $\text{CH}_2\text{Cl}_2$ . (c) dioxane-HCl. (d) iPO/ $\text{H}_2\text{O}$ .

Scheme 2<sup>a</sup>

<sup>a</sup> Reagents and conditions: (a) iPO/ $\text{H}_2\text{O}$ .

Scheme 3<sup>a</sup>

<sup>a</sup> Reagents and conditions: (a) thiourea/MEK (b) NaH/DMF (c) MCPBA/ $\text{CH}_2\text{Cl}_2$  (d) dioxane-HCl.

investigations within the core family of novel sulfonylpyridazinones.

## Chemistry

The synthetic route for the phenyl-substituted analogues is shown in Scheme 1. Benzenethiols with desired substituents, **2**, were reacted with 3-chloro-6-methoxy-pyridazine, **1**, in the presence mild or strong bases, to obtain compound **3**. Controlled or complete sulfoxidation using MCPBA, followed by hydrolysis of the resulting **4** or **5**, in the presence of aqueous HCl, gave **7** or the target compound, **8**.<sup>22</sup> Hydrolysis of **3** under similar conditions gave **6**. Compound **8** was also prepared in one step starting from aryl sulfinic acid salt, **11**, as shown in Scheme 2. **8j** was prepared by the standard palladium-catalyzed coupling of 4-bromophenyl sulfone, **8b**, with phenylboronic acid.

Sulfonylmethyl compounds **15** were prepared starting from the known 3-mercapto-4-methoxy pyridazine<sup>23</sup> **12** and allowed to react with benzyl halides **13** (X = Cl, Br), to obtain the sulfenylmethyl compound **14** (Scheme 3). Peracid oxidation of **14** followed by acid hydrolysis of the resulting **14** ( $n = 2$ ) gave the target compounds **15**<sup>24</sup> (cf. Scheme 1).

Scheme 4 depicts the method used for the preparation of pyridazinones with a heterocyclic side chain. Lithiated heterocycle prepared from deprotonation of heterocycles **17** with  $n\text{-BuLi}$  was added to the sulfonyl fluoride<sup>23</sup> **16** to obtain **18**, which was hydrolyzed under acidic conditions to obtain the target compound **19**. Reversing the order of addition of the reactants significantly improved the yield of **19**. Depending on the access to mercapto heterocycles, Scheme 1 could also be used. For example, the parent indole **19a** was prepared

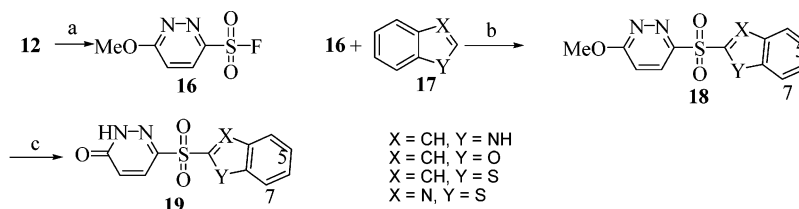
starting with 2-mercaptoindole. In the case of other indoles, sulfonyl-protected derivatives (cf. **17**, Y =  $\text{NSO}_2\text{-Ph}$ ) were used in the lithiation step. The  $\text{SO}_2\text{Ph}$  was freed by base hydrolysis prior to unmasking the methoxy group to obtain the pyridazinones with indole side chains.

## Biology

Full details of the biological methods employed are included in the Experimental Section. Primary in vitro screening of potential inhibitors was conducted using human recombinant AR. Coefficient of variation for the screening assay based on 21 determinations each with inhibitors zopolrestat, sorbinil, and compound **18m** was 102%. Selectivity vs aldehyde reductase (ALR) was determined using rat kidney ALR and a highly specific AR inhibitor.<sup>25</sup> Sufficiently potent in vitro AR inhibitors were evaluated in streptozotocin-induced diabetic rats with two protocols. The acute test (also referred to as prevention test), a 27-h model with tid dosing, measured the preventive ability of the inhibitors to normalize the excess accumulation of metabolites, sorbitol as well as fructose, in the sciatic nerve. The chronic test, employing once-a-day dosing of the inhibitor for 5 days following 1 week of untreated diabetes, assessed the potential of acute test active inhibitors to normalize already elevated levels of the same metabolites in the same tissue. The blood glucose levels in diabetic control rats in the acute and chronic tests, respectively, were in the range of 300–350 and 600–650 mg/dL. As a general approach, unless an inhibitor nearly normalized either sorbitol or fructose in the acute test, it was not progressed to the chronic test. Potent activity in the chronic test was taken as an encouraging sign that the inhibitor may show good pharmacokinetics in other species, including humans. Selected inhibitors were tested for effect on accumulation of sorbitol in lens, in both test protocols. All in vivo inhibition responses included in Tables 1–3 were statistically significant at  $p \leq 0.05$  vs diabetic control values, except for values indicated. This is the first full report in which nerve fructose has been included as a critical part of the primary in vivo screening criteria for blocking flux through the polyol pathway, rather than merely sorbitol, as has routinely been done until now.

## Results and Discussion

High-throughput screening of internal libraries of compounds has proved to be an expedient avenue to search for potential new leads. However, the eventual success in delivering potential clinical candidates with

Scheme 4<sup>a</sup>

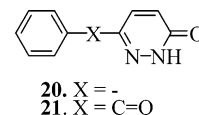
<sup>a</sup> Reaction conditions: (a)  $\text{KHF}_2/\text{Cl}_2(\text{g})\text{-MeOH}/\text{H}_2\text{O}$ . (b)  $n\text{-BuLi}$ , THF,  $-78^\circ\text{C}$ . (c) dioxane/HCl (concd).

satisfactory pharmaceutical properties appears to hinge, in large part, on the initial criteria set for identification of leads and working strategies employed for optimization of structure–activity relationships (SAR). Our target was low molecular weight non-carboxylic acid, non-hydantoin structures with no readily discernible toxic pharmacophore and with good in vitro activity vs human r-AR at  $\leq 1 \mu\text{M}$ . Our extensive library yielded only one hit with this set of credentials, with an  $\text{IC}_{50}$  of  $0.6 \mu\text{M}$ , except that the compound was registered in the file with structure **10**, featuring a very unattractive, labile bis-sulfone, signaling potential chemical stability and safety issues. It could have been easily rejected to terminate the project, but the length of time spent on in vitro screening justified at least a preliminary in vivo test of the compound, against the conventional sorbitol end point. Surprisingly, **10** showed good sorbitol inhibition activity in the sciatic nerve of diabetic rats in the acute test. To our knowledge of the ARI literature and in our own experience, this was the first time that a compound with no measurable  $\text{pK}_a$ , specifically on the acidic side, showed both in vitro and in vivo activities. It was hard to reconcile the new finding with the repository of X-ray structures of the AR–cofactor–ARI complexes, where every ARI is lodged deep inside the anion well.<sup>26</sup> A simple solubility test in aqueous sodium hydroxide confirmed that the inhibitor was at least weakly acidic. Acidification of the basic solution gave a precipitate as would have been expected, and serendipitously, the precipitate was sufficiently crystalline for a single-crystal X-ray, which proved beyond a doubt that the inhibitor was indeed 6-phenylsulfonylpyridazin-2H-3-one, **8**.<sup>22</sup> It has low molecular weight (236) and is weakly acidic ( $\text{pK}_a$ , 7.1). In our new screening paradigm, it normalized elevated nerve sorbitol levels by 95% and fructose levels by 89%, albeit at a high dose of 300 mg/kg, in the sciatic nerve of acutely diabetic rats. In subsequent dose titration in the acute test, **8** showed  $\text{ED}_{50}$ s of 15 and 25 mg/kg, against sorbitol and fructose end points, respectively. Just to trace the genesis of structure misassignment, it is instructive to see how it was prepared. Reaction of 3,6-dichloropyridazine gives the corresponding bis-sulfide, which when oxidized with peracid leads to the bis-sulfone. However this labile bis-sulfone undergoes hydrolysis under conditions of aqueous workup, resulting in **8** (Scheme 1). Strong support for this view comes from the rapid in situ hydrolysis of the electron-withdrawing 3-Cl, following peracid oxidation of 3-chloro-8-phenylsulfonylphthalazine to the phthalazinone analogue **8y** (see Experimental Section).

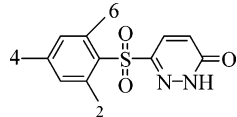
With a novel lead of desired profile in hand, our goal was to seek an inhibitor at least 10 times more potent than zopolrestat in the chronic diabetic rat model against the targeted nerve fructose end point ( $\text{ED}_{90}$ ),

through a systematic SAR pursuit around **8**. As an expedient strategy toward the objective, the resource demanding in vivo tests were run at a maximum dose no higher than 20 mg/kg, with only a very few exceptions. A down side of this strategy was that sharper SAR insights into the relative ranking of inhibitors that were not sufficiently potent at 20 mg/kg could not be discerned.

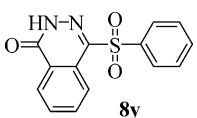
Because the phthalazinone template had already been deployed to design potent ARIs such as ponalrestat and zopolrestat, sulfonyl phthalazinone **8y**, with a 4<sup>1,5</sup> benzo substituent (see Table 1), was prepared very early on, but it showed little AR inhibition activity. Consequently, the first phase of our investigation focused on SAR, which encompassed deletion of the  $\text{SO}_2$  linker, replacement of the linker by CO, extension of the linker by  $\text{CH}_2$  (i.e.  $\text{SO}_2\text{-CH}_2$ ), and substituents on the phenyl ring. The first two modifications, **20**<sup>27</sup> and **21**,<sup>28</sup> showed no AR inhibition activity, even at  $10 \mu\text{M}$ . Furthermore, the methoxy sulfone **5** ( $n = 2$ , no measurable  $\text{pK}_a$ ) also showed no AR inhibition activity, even at  $32 \mu\text{M}$ .



We will now discuss SAR relative to substituents on the phenyl ring of **8** and homologues of **8** featuring the  $\text{SO}_2\text{-CH}_2$  linker. Phenyl substituents were chosen to probe the influence of orientation, lipophilicity, electron withdrawal, electron release, and steric bulk. In general, compact, electron-withdrawing F and Cl substituents that are reasonably lipophilic gave potent compounds both in vitro and in vivo. Compounds with one Cl (**8c–e**), two Cl (**8k–o**), and one Cl with one F (**8s**), especially at the 2- and 2,4-positions, showed the most attractive in vivo activity. Among these, **8l** was the best (vide infra). However, **8t**, which features the effective 2F, 4Br substituent pattern present in ponalrestat,<sup>29</sup> zenarrestat,<sup>11</sup> and minalrestat,<sup>19</sup> was less potent than **8l** in vivo.  $\text{IC}_{50}$ s for this group of compounds were in the range of 50–400 nM. Electron-releasing substituents (e.g., OMe and Me, **8h** and **8i**) and bulky groups, especially at the 2-position (e. g., Ph, **8j**), had unfavorable effect on in vitro potency. However, unlike **8j**, which could have many degrees of rotation around the 2-phenyl bond, rigid naphthalenes, **8w** and **8x**, were more potent than **8**, suggesting the scope of permissible space for activity. Table 1 summarizes SAR in the phenylsulfonyl pyridazinone series. 6-(2,4-Dichloro-phenylsulfonyl)-2H-pyridazin-3-one, **8l** ( $\text{pK}_a$ , 6.9;  $\text{IC}_{50}$ , 190 nM), was the most potent inhibitor in the chronic test; it was 2 times more potent than zopolrestat in normalizing both sciatic

**Table 1.** In Vitro and in Vivo Data for Phenyl-Substituted Sulfonylpyridazinones


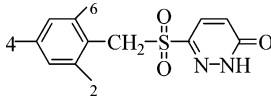
compd	sub.	IC <sub>50</sub> (nM)	dose (mg/kg)	% inhibition <sup>a</sup>			
				acute test		chronic test	
				s	f	s	f
<b>8</b>		600	50	95	74		
			25	73	49		
			10	40	14 <sup>f</sup>		
			ED <sub>50</sub> <sup>h</sup>	15	25		
<b>8a</b>	2-Br	210	50	55	<i>b</i>		
<b>8b</b>	4-Br	350	50	26 <sup>f</sup>			
<b>8c</b>	2-Cl	170	20	101	81		
			10	96	68		
<b>8d</b>	3-Cl	240	<i>c</i>				
<b>8e</b>	4-Cl	380	10	65	52		
<b>8f</b>	2-F	540	20	91	56		
			10	79	34		
<b>8g</b>	4-F	474	50	81	<i>b</i>	74	<i>b</i>
<b>8h</b>	4-OMe	2.0 μM	<i>c</i>				
<b>8i</b>	4-Me <sup>d</sup>	1.9 μM	<i>c</i>				
<b>8j</b>	2-Ph	2.2 μM	<i>c</i>				
<b>8k</b>	2,3-Cl <sub>2</sub>	55	20	98	<i>b</i>	89	
			10	77	<i>b</i>		
			5	55	<i>b</i>	81	
<b>8l</b>	2,4-Cl <sub>2</sub>	190	ED <sub>50</sub>	0.8	3	<i>g</i>	
<b>8m</b>	2,5-Cl <sub>2</sub>	73	20	79	67		
			10	65	36		
<b>8n</b>	2,6-Cl <sub>2</sub>	50	30	81	<i>b</i>		
			20			75	<i>b</i>
<b>10</b>				58	<i>b</i>	50	<i>b</i>
<b>8o</b>	3,4-Cl <sub>2</sub>		20	98	85		
			10	84	60		
<b>8p</b>	3,5-Cl <sub>2</sub>		20	91	49	73	38
			5	68	32	63	30
<b>8q</b>	2,3-F <sub>2</sub>	390	30			<i>b</i>	81
			10			<i>b</i>	50
<b>8r</b>	2,4-F <sub>2</sub>	870	<i>c</i>				
<b>8s</b>	2-Cl, 4-F	280	20	106	97		
			10	95	87		
<b>8t</b>	2-F, 4-Br	140	10	81	67		
<b>8u</b>	3-CF <sub>3</sub>	175	20	45	17 <sup>f</sup>		
<b>8v</b>	4-CF <sub>3</sub>	360	20	67	24 <sup>f</sup>		
			10	44	10 <sup>f</sup>		
<b>8w</b>	2,3-benzo	150	20	95	55	70	43
			10	88	49	60	31
<b>8x</b>	3,4-benzo	360	20			74	51

sorbitinil	140	<i>e</i>	<i>g</i>
zopolrestat	4	<i>e</i>	

<sup>a</sup> s = sorbitol. f = fructose. <sup>b</sup> Not measured. <sup>c</sup> Not tested. <sup>d</sup> Chem. Abstr. 1960, 5714. <sup>e</sup> See Figures 1–3 for in vivo comparative data. <sup>f</sup> Not statistically significant at  $p \leq 0.05$ . <sup>g</sup> See Figures 3–5. <sup>h</sup> In mg/kg.

nerve sorbitol (ED<sub>90</sub>, 5 vs 10 mg/kg) and fructose (ED<sub>90</sub>, 20 mg/kg vs ~40 mg/kg) levels. Even though **8l** is nearly 25-fold less potent than zopolrestat (IC<sub>50</sub>, 190 nM vs 4 nM), it is markedly more effective than zopolrestat in suppressing lens sorbitol levels (94% vs 30% at 20 mg/kg), suggesting that the new class of ARIs penetrate the diabetic target tissues far more efficiently than a typical carboxylic acid ARI (cf. Figures 3–5). Because xenobiotics can penetrate into the avascular lens tissue from systemic blood only by diffusion of uncharged species,

**Table 2.** In Vitro and in Vivo Data for Benzyl-Substituted Sulfonylpyridazinones


compd	sub.	IC <sub>50</sub> (nM)	dose (mg/kg)	% inhibition <sup>a</sup>			
				acute test		chronic test	
				s	f	s	f
<b>15</b>		600	60	73	<i>b</i>		
<b>15a</b>	2-Cl	118	<i>c</i>				
<b>15b</b>	2-F	422	<i>c</i>				
<b>15c</b>	2-CF <sub>3</sub>	500	<i>c</i>				
<b>15d</b>	3-CF <sub>3</sub>	72	20	88	70	65	42
<b>15e</b>	2, 3-Cl <sub>2</sub>	35	20	65	48		
<b>15f</b>	2,6-Cl <sub>2</sub>	52	10	42	24 <sup>d</sup>		
<b>15g</b>	2,3-F <sub>2</sub>	257	20	82	51		
<b>15h</b>	2-F, 4-Br	667	<i>c</i>				
<b>15i</b>	2-Cl, 6-F	26	20	42	45		
<b>15j</b>	2F, 3-Cl	54	20	74	64		
<b>15k</b>	2-F, 3-CF <sub>3</sub>	44	20	61	56		

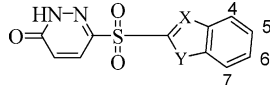
<sup>a</sup> s = sorbitol. f = fructose. <sup>b</sup> Not measured. <sup>c</sup> Not tested. <sup>d</sup> Not statistically significant at  $p \leq 0.05$ .

it is understandable why **8l**, with a much higher pK<sub>a</sub> than zopolrestat (6.9 vs 3.8), would be more effective.

We investigated the impact of increasing the length of the linker by one methylene group, as in **15**. SAR exploration was guided by experience in the phenyl series, but it was confounding. While several halogen-substituted compounds were found to be more potent in vitro than the best inhibitors in the phenyl series, they were, by and large, less potent in vivo, and no inhibitor more potent than **8l** could be identified. While we did not study the pharmacokinetics/metabolism issues in this series, we surmise that metabolic oxidation at the methylene carbon (common to all inhibitors) may have been a key factor for the lack of good correlation between in vitro and in vivo potency.

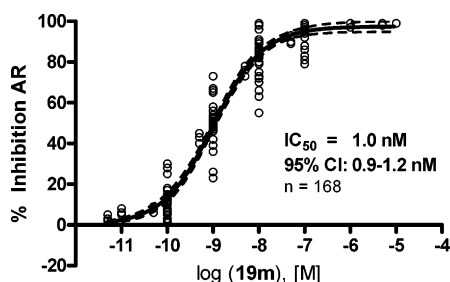
As we had not yet achieved our in vivo potency goal (10 times zopolrestat), we explored activity-potentiating replacements for the phenyl in **8** with selected heterocycles. On the basis of previous SAR experience with zopolrestat<sup>30a</sup> and related analogues,<sup>30b</sup> the X-ray structure information from the AR–NADPH(NADP<sup>+</sup>)–zopolrestat ternary complex,<sup>31</sup> and a literature example, **20** (M-16209),<sup>32</sup> we targeted a new family of compounds of general formula **19**.

The rank order of in vitro potency (IC<sub>50</sub>), at least numerically, among the parent heterocycles was benzofuran (**19h**) (150 nM) ~ benzothiofuran (**19w**) (180 nM) > benzothiazole (**19z**) (450 nM) > indole (**19a**) (590 nM). None had the desired in vivo potency, and also a number of SAR probes around **19a** did not improve the status quo. However, on the basis of the in vitro potency of **19h**, literature data for **20**, and the potential vulnerability of **19w** for metabolic oxidation of the sulfur atom, we decided to focus SAR around the benzofuran **19h**. We thought that we needed to increase lipophilicity for better tissue penetration. There is very sparse knowledge about the metabolism of benzofuran with an electron-withdrawing group at the 5-position. Nevertheless, it appeared that the strategy of blocking the highly electrophilic 5-position with a lipophilic Cl substituent would be a good probe to address both issues. More significantly, zopolrestat with a 5-CF<sub>3</sub> on the benzothia-

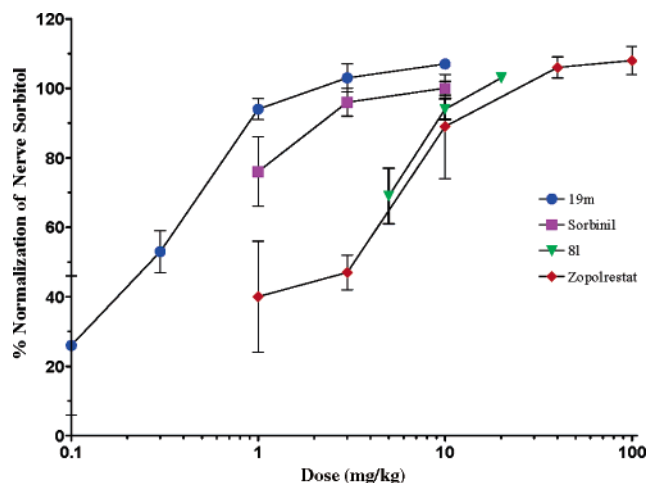
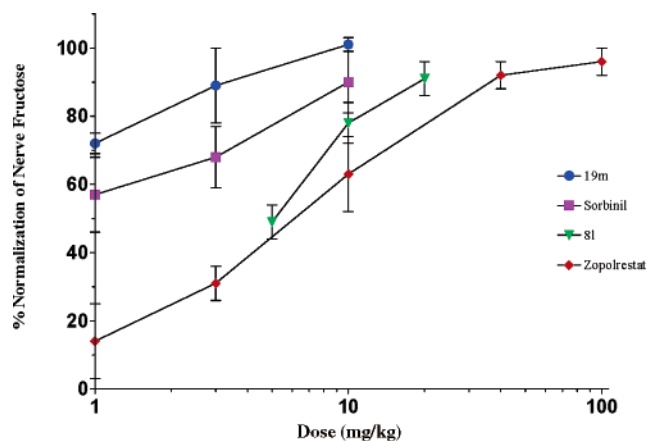
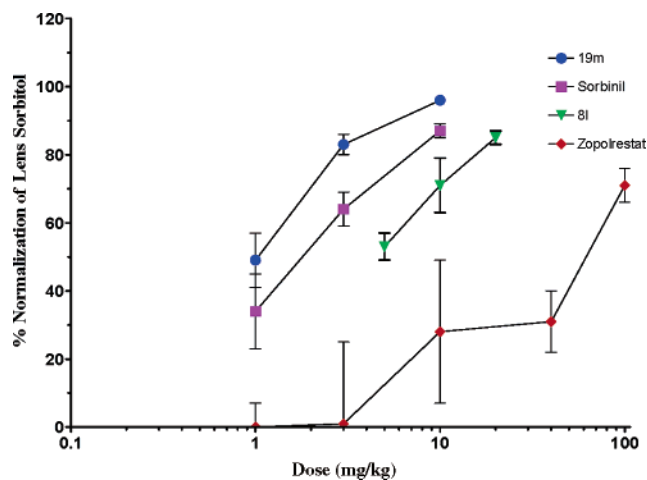
**Table 3.** In Vitro and in Vivo Data for Sulfonylpyridazinones with Heterocyclic Side Chains


compd	X	Y	sub.	IC <sub>50</sub> (nM)	dose (mg/kg)	% inhibition <sup>a</sup>			
						acute test		chronic test	
						s	f	s	f
<b>19a</b>	CH	NH		590	20	100	82	67	50
<b>19b</b>	CH	NH	5-Cl	1.1 $\mu$ M	<i>c</i>				
<b>19c</b>	CH	NH	6-Cl	645	<i>c</i>				
<b>19d</b>	CH	NH	7-Cl	450	20	40	44		
<b>19e</b>	CH	NH	6-F	1.4 $\mu$ M	<i>c</i>				
<b>19f</b>	CH	NH	5,6-OCH <sub>2</sub> O	3.8 $\mu$ M	<i>c</i>				
<b>19g</b>	CH	NH	5,7-Cl <sub>2</sub>	200	<i>c</i>				
<b>19h</b>	CH	O		150	10	<i>b</i>	34		
<b>19i</b>	CH	O	5-Cl	25	10	<i>b</i>	39		
<b>19j</b>	CH	O	3-Me	140	20	<i>b</i>	56		
					10	<i>b</i>	43		
<b>19k</b>	CH	O	5-OMe	230	20	49	34		
<b>19l</b>	CH	O	5, 7-Cl <sub>2</sub>	87	10	32	39		
<b>19m</b>	CH	O	3-Me, 5-Cl	1	ED <sub>50</sub> <sup>f</sup>	0.2	0.8	<i>e</i>	
<b>19n</b>	CH	O	3-Me, 6-Cl	190	10	40	28 <sup>d</sup>		
<b>19o</b>	CH	O	3-Me, 5-F	3	10	84	62	100	90
					3	66	42	86	64
					1	47	11 <sup>d</sup>	52	17 <sup>d</sup>
					ED <sub>50</sub>	1.2	5.8	1	2.4
<b>19p</b>	CH	O	3-Me, 5-CF <sub>3</sub>	5	10	101	97	102	100
					3	91	79	95	81
					1	43	19 <sup>d</sup>	75	54
					ED <sub>50</sub>	1.3	2.0	<1	1
<b>19q</b>	CH	O	3, 5-Me <sub>2</sub>	13	10	21 <sup>d</sup>	18 <sup>d</sup>	<i>c</i>	
<b>19r</b>	CH	O	3-Et, 5-Cl	6	10	<i>b</i>	<i>b</i>	48	24 <sup>d</sup>
<b>19s</b>	CH	O	3- <sup>i</sup> Pr, 5-Cl	92	10	<i>b</i>	<i>b</i>	48	14 <sup>d</sup>
<b>19t</b>	CH	O	3-Ph	23	<i>c</i>				
<b>19u</b>	CH	O	3-(4-F)-Ph	49	10	66	50	<i>c</i>	
<b>19v</b>	CH	O	3-Ph, 5-Cl	34	20	27 <sup>d</sup>	20 <sup>d</sup>	<i>c</i>	
<b>19w</b>	CH	S		180	20	46	22 <sup>d</sup>	<i>c</i>	
<b>19x</b>	CH	S	5-Me	160	20	<i>b</i>	7 <sup>d</sup>	<i>c</i>	
<b>19y</b>	CH	S	3Me, 5-Cl	55	10	83	51	<i>c</i>	
					3	49	29 <sup>d</sup>	<i>c</i>	
<b>19z</b>	S	N		450	<i>c</i>				

<sup>a</sup> s = sorbitol. f = fructose. <sup>b</sup> Not measured. <sup>c</sup> Not tested. <sup>d</sup> Not statistically significant at  $p \leq 0.05$ . <sup>e</sup> See Figures 3–5. <sup>f</sup> In mg/kg.

**Figure 2.** In vitro AR inhibition dose–response.

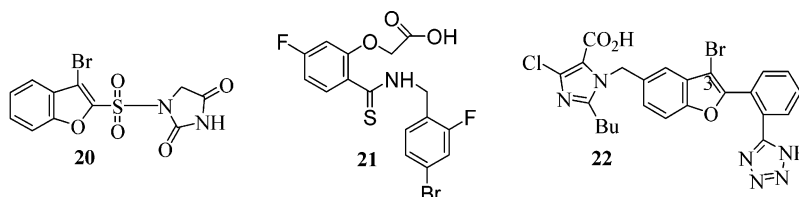
zole was >20 times more potent than its 6-CF<sub>3</sub> congener in vitro, and it turns out that the strategically placed 5-CF<sub>3</sub> cooperatively aided in the binding of zopolrestat within the anion well, through powerful hydrogen-bond-accepting fluorine atoms, two of which are in close contact with Thr113 and Cys303 in the X-ray structure of AR–cofactor–zopolrestat ternary complex.<sup>31</sup> Also, a similar strong interaction between the bromine in the ARI **21** (IDD 594) and Thr113 has been depicted.<sup>26</sup> So hydrogen-bond-accepting halogens at the 5-position of the benzofuran side chain became immediate targets. **19i** (IC<sub>50</sub>, 25 nM) was found to be more potent in vitro

**Figure 3.** Chronic test: nerve sorbitol data.**Figure 4.** Chronic test: nerve fructose data.**Figure 5.** Chronic test: lens sorbitol data.

than **19h**, but it was still not very potent in vivo, even though it gave good serum levels when administered orally (data not shown).

Faced with a potency impasse, it is not uncommon for medicinal chemists to draw lessons from disparate drug series. We noticed that whenever benzofuran had been employed in other medicinal chemistry projects, a 3-substituent had played a remarkable role in enhancing in vivo potency. In addition to a 3-bromo substituent in **20** (Chart 2),<sup>32</sup> we were particularly impressed by the role of the same substituent in the benzofuran-based

## Chart 2



AII blocker **22** (GR-117289)<sup>33</sup> in providing efficacy in blood pressure lowering, in rat models.

So we appended a 3-substituent to the best benzofuran in hand, **19i**. We preferred to incorporate a methyl group, rather than an additional halogen atom, leading to **19m**, which is one of the most potent ARIs yet described in the literature. Before we return to the detailed laboratory profile of **19m**, we turn our attention to additional SAR around **19m**. Replacing the 5-Cl in **19m** by F or CF<sub>3</sub> led to inhibitors **19o** or **19p**, respectively, which retained a significant portion of the in vitro and in vivo potencies of **19m**, but neither was quite equal to **19m**, although **19p** was closer to **19m**. On the other hand, the 5-Me congener **19q** was considerably less potent than **19m**, **19o**, or **19p** in vivo. As speculated above, the 6-Cl analogue **19n** was markedly less potent than **19m** (IC<sub>50</sub>, 0.8 nM vs 190 nM), suggesting perhaps a nonoptimum orientation for the 6-Cl to interact with a hydrogen-bond-accepting residue in the AR. Again, it is interesting to note that, even in the zopolrestat series, the 6-Cl congener was less potent (10 times) than the 5-Cl congener. The progressively more lipophilic 3-substituted compounds **19r–v** were all less potent than **19m**. Among these, the least lipophilic, **19r**, was the most potent. The observed in vivo potency difference between **19p** and **19r** with nearly the same IC<sub>50</sub>s is rather difficult to explain, except to invoke facile biohydroxylation of the ethyl group, leading to greater clearance and/or decreased sciatic nerve penetration. The first possibility has support from the experimentally measured lower activation energy for P450 oxidation of ethyl benzene over toluene and the reported lower CYP2 K<sub>m</sub> for ethyl benzene vs toluene.<sup>34,35</sup> The early choice of focusing SAR on the benzofuran template is borne out by a comparison of benzothiophene **19y** with **19m**. Even though **19y** has the same substitution pattern as in **19m**, it is ~50-fold less potent than **19m** in vitro.

The best inhibitor, **19m** (CP-744809), was selected for further laboratory characterization. Its IC<sub>50</sub> vs r-human AR is 1 nM (*n* = 168, Figure 2). For its low molecular weight (324), it is the most potent AR inhibitor in vitro. In a side-by-side evaluation, its ED<sub>90</sub> for normalization of fructose in the chronic test (Figure 4) is lower than that of zopolrestat (13 times) and of sorbinil (3 times). The dose–response of **19m** for inhibition of sorbitol (Figure 3) and fructose reiterates the greater sensitivity for sorbitol over fructose and should raise caution in targeting just sorbitol as a robust marker of flux through the polyol pathway. Inhibitor **19m**, in contrast to zopolrestat, shows remarkable potency in suppressing sorbitol in lens (Figure 5). In fact, it is the most potent inhibitor in lens relative to comparators, including sorbinil, the previous best in our hands. Recently, it has been reported that **19m** shows positive effects in the diabetic kidney. In a diabetic rat model, it shows a near normalization of elevated (2.5-fold) urinary albumin

output relative to normal rats.<sup>36</sup> Selectivity profiling of **19m** against aldehyde reductase<sup>37</sup> and alcohol,<sup>38</sup> fructose,<sup>39</sup> and sorbitol dehydrogenases<sup>9b</sup> showed respectively the following IC<sub>50</sub>s (nM): 930, 18 000, 25 000, and > 100 000. This selectivity profile makes CP-744,809, to our knowledge, the most selective orally active ARI. Its pK<sub>a</sub>, log *P*, and log *D* (pH 7.4) respectively are 6.9, 3.05, and 2.46. A higher log *D*/log *P* value of 0.81, for **19m**, is in stark contrast with the value of 0.16, for zopolrestat,<sup>30a</sup> and is consistent with more effective penetration of **19m** into the lens tissue. It is very well absorbed in rats, with oral bioavailability of 98% (plasma C<sub>max</sub>, 9 ± 3 μg/mL at 2 mg/kg, po), and shows a favorable plasma *t*<sub>1/2</sub> (26 ± 3 h). These desirable physicochemical and pharmacokinetic properties of **19m**, taken together with its stability toward P450 enzymes and excellent Caco-2 transcellular permeability (>10<sup>-5</sup> cm/s), bode well for potential once-a-day dosing in the clinic.

## Conclusion

High-throughput screening of internal libraries of compounds targeted toward a structurally distinct non-hydantoin, non-carboxylic acid ARI, with potential to robustly block the flux through the polyol pathway, yielded a weak inhibitor, **8**. Nearly complete normalization of elevated fructose (rather than just sorbitol) levels (ED<sub>90</sub>) in the sciatic nerve of rats with established diabetes was used as the primary biochemical marker for effective blockade of flux. A systematic SAR pursuit around **8**, with initial focus on the phenyl ring substitution, yielded **81**, which was 2 times more potent than zopolrestat in the chronic test against the fructose end point. Spurred by this significant finding and applying lessons learned from literature on extant ARIs, especially zopolrestat, and monitoring the profile of newly prepared analogues for lipophilicity (both log *P* and *D*), movement across Caco-2 cell monolayer via transcellular mechanism, and pharmacokinetics in rats led to the title compound 6-(5-chloro-3-methylbenzofuran-2-sulfonyl)-2*H*-pyridazin-3-one, **19m**. It is a novel, highly selective ARI with unprecedented in vitro potency (1 nM, *n* = 168) and remarkable potency in the sciatic nerve, as well as in the lens of chronically diabetic rats, in normalizing polyol metabolites. It is reported to show positive effects in a diabetic rat model of proteinuria, and it is well absorbed in diabetic rats with sustained plasma *t*<sub>1/2</sub> of 26 ± 3 h.

## Experimental Section

All target compounds gave elemental analyses data for C, H, and N in compliance with the commonly acceptable range (see Supporting Information). All reactions were carried out using commercial grade reagents and solvents. The <sup>1</sup>H NMR spectra were recorded on a Varian Unity Inova 400 MHz spectrometer at 400 MHz with chemical shifts (δ) reported in ppm downfield relative to tetramethylsilane internal standard.



Anhydrous  $\text{Na}_2\text{SO}_4$  was used as the drying agent. Chemical abbreviations: MCPBA = *m*-chloroperoxybenzoic acid.

**6-(3-Chlorobenzenesulfonyl)-2H-pyridazin-3-one (8d).**

**Step 1.** Sodium metal (218 mg, 9.5 mmol) was dissolved in MeOH (10 mL). 3-Chlorothiophenol (1.12 g, 7.7 mmol) was added and the mixture stirred for 1 h at room temperature. The excess MeOH was evaporated and to the dry residue were added toluene (20 mL) and 3-chloro-6-methoxy-pyridazine (1.1 g, 7.7 mmol). The reaction mixture was refluxed for 4 h, cooled to room temperature, and then poured into  $\text{H}_2\text{O}$  (30 mL). The pH of the solution was first adjusted to 10 with 20% KOH and extracted with EtOAc. The aqueous layer from the extraction was collected. The aqueous portion was acidified to pH 3 with concentrated HCl acid and then extracted with EtOAc. The EtOAc extract was evaporated and the residue was purified by silica gel chromatography to afford 3-(3-chloro-phenylsulfanyl)-6-methoxy-pyridazine.

**Step 2.** A mixture of 3-(3-chlorophenylsulfanyl)-6-methoxy-pyridazine (529 mg, 1.5 mmol), MCPBA (760 mg, 4.4 mmol), and  $\text{CHCl}_3$  (20 mL) was prepared and stirred at room temperature for 2 h. The reaction mixture was diluted with 5% sodium thiosulfate (20 mL) followed by  $\text{H}_2\text{O}$  (30 mL). The  $\text{CHCl}_3$  layer was collected, dried, and filtered, and the dried  $\text{CHCl}_3$  portion was evaporated to dryness. The resulting solid residue was purified by silica gel chromatography (3:1 hexane/EtOAc as eluent) to obtain 3-(3-chloro-benzenesulfonyl)-6-methoxy-pyridazine (29%, 173 mg).

**Step 3.** A mixture of 3-(3-chlorobenzenesulfonyl)-6-methoxy-pyridazine (148 mg, 0.52 mmol), dioxane (2 mL), and concentrated HCl (0.5 mL) was prepared and refluxed for 30 min. The reaction mixture was then evaporated to dryness and the residue was extracted with EtOAc. The EtOAc mixture was collected, dried, and filtered, and the filtrate was evaporated to dryness to afford **8d** as white solid (38%, 61 mg): mp 222–223 °C;  $^1\text{H NMR}$ ,  $\text{DMSO-}d_6$ ,  $\delta$  7.11 (d,  $J$  = 8 Hz, 1H), 7.74 (s, 1H), 7.86–8.04 (m, 4H), 13.86 (s, 1H). The following examples were prepared from the appropriate starting materials in a manner analogous to the method of example **8d**.

**6-(2-Bromobenzenesulfonyl)-2H-pyridazin-3-one (8a)** (38%): mp 210–213 °C;  $^1\text{H NMR}$ ,  $\text{DMSO-}d_6$ ,  $\delta$  7.15 (d,  $J$  = 8 Hz, 1H), 7.72 (m, 2H), 7.91 (m, 1H), 8.04 (d,  $J$  = 8 Hz, 1H), 8.79 (m, 1H), 13.80 (s, 1H).

**6-(4-Bromobenzenesulfonyl)-2H-pyridazin-3-one (8b)** (21%): mp >200 °C;  $^1\text{H NMR}$ ,  $\text{DMSO-}d_6$ ,  $\delta$  7.08 (d,  $J$  = 9 Hz, 1H), 7.77 (d,  $J$  = 9 Hz, 2H), 7.98 (m, 2H), 7.98 (m, 1H), 13.82 (s, 1H).

**6-(2-Chlorobenzenesulfonyl)-2H-pyridazin-3-one (8c)** (28%): mp 222 °C;  $^1\text{H NMR}$  (DMSO, 300 MHz)  $\delta$  7.25 (d,  $J$  = 8 Hz, 1H), 7.72 (m, 2H), 7.91 (m, 1H), 8.04 (d,  $J$  = 8 Hz, 1H), 8.91 (m, 1H), 13.80 (s, 1H).

**6-(4-Chlorobenzenesulfonyl)-2H-pyridazin-3-one (8e)** (35%): mp >220 °C;  $^1\text{H NMR}$ ,  $\text{DMSO-}d_6$ ,  $\delta$  7.08 (d,  $J$  = 9 Hz, 1H), 7.77 (d,  $J$  = 9 Hz, 2H), 7.98 (m, 2H), 7.98 (m, 1H), 13.82 (s, 1H).

**6-(4-Fluorobenzenesulfonyl)-2H-pyridazin-3-one (8g)** (37%): mp >225 °C;  $^1\text{H NMR}$ ,  $\text{DMSO-}d_6$ ,  $\delta$  7.08 (d,  $J$  = 9 Hz, 1H), 7.77 (d,  $J$  = 9 Hz, 2H), 7.98 (m, 2H), 7.98 (m, 1H), 13.82 (s, 1H).

**6-(4-Methoxybenzenesulfonyl)-2H-pyridazin-3-one (8h)** (45%): mp 111–113 °C;  $^1\text{H NMR}$ ,  $\text{DMSO-}d_6$ ,  $\delta$  3.87 (s, 3H), 7.06 (d,  $J$  = 9 Hz, 1H), 7.20 (d,  $J$  = 8 Hz, 1H), 7.90 (d,  $J$  = 8 Hz, 1H), 7.95 (d,  $J$  = 9 Hz, 1H), 13.71 (b, 1H).

**6-(2,3-Dichlorobenzenesulfonyl)-2H-pyridazin-3-one (8k)** (76%): 224–225 °C;  $^1\text{H NMR}$ ,  $\text{DMSO-}d_6$ ,  $\delta$  7.13 (d,  $J$  = 9 Hz, 1H), 7.60 (dd,  $J$  = 2 Hz, 8 Hz, 1H), 7.87 (dd,  $J$  = 2 Hz, 8 Hz, 1H), 8.02 (d,  $J$  = 9 Hz, 1H), 8.33 (m, 1H), 13.86 (s, 1H).

**6-(2,4-Dichlorobenzenesulfonyl)-2H-pyridazin-3-one (8l)** (87%): mp 202–203 °C;  $^1\text{H NMR}$ ,  $\text{DMSO-}d_6$ ,  $\delta$  7.15 (d,  $J$  = 9 Hz, 1H), 7.81 (dd,  $J$  = 8 Hz, 1 Hz, 1H), 8.03 (m, 2 H), 8.25 (d,  $J$  = 9 Hz, 1H), 13.88 (b, 1H).

**6-(2,5-Dichlorobenzenesulfonyl)-2H-pyridazin-3-one (8m)** (72%): mp 229–232 °C;  $^1\text{H NMR}$ ,  $\text{DMSO-}d_6$ ,  $\delta$  7.15 (d,

$J$  = 8 Hz, 1H), 7.81 (d,  $J$  = 9 Hz, 1H), 8.0 (dd,  $J$  = 8 Hz, 2 Hz, 1H), 8.06 (d,  $J$  = 9 Hz, 1H), 8.20 (d,  $J$  = 2 Hz, 1H), 13.89 (b, 1H).

**6-(2,6-Dichlorobenzenesulfonyl)-2H-pyridazin-3-one (8n)** (81%): mp 219–220 °C;  $^1\text{H NMR}$ ,  $\text{DMSO-}d_6$ ,  $\delta$  7.15 (d,  $J$  = 10 Hz, 1H), 7.74 (m, 3H), 8.0 (d,  $J$  = 10 Hz, 1H), 13.80 (b, 1H).

**6-(3,4-Dichlorobenzenesulfonyl)-2H-pyridazin-3-one (8o)** (55%): mp 166–168 °C;  $^1\text{H NMR}$ ,  $\text{DMSO-}d_6$ ,  $\delta$  7.09 (d,  $J$  = 9 Hz, 1H), 7.74 (m, 2H), 8.0 (d,  $J$  = 9 Hz, 1H), 8.21 (d,  $J$  = 2 Hz, 1H), 13.87 (s, 1H).

**6-(3,5-Dichlorobenzenesulfonyl)-2H-pyridazin-3-one (8p)** (42%): mp 231–232 °C;  $^1\text{H NMR}$ ,  $\text{DMSO-}d_6$ ,  $\delta$  7.01 (d,  $J$  = 9 Hz, 1H), 7.80 (d,  $J$  = 9 Hz, 1H), 7.89 (s, 1H), 8.35 (s, 2H), 13.76 (b, 1H).

**6-(2,3-Difluorobenzenesulfonyl)-2H-pyridazin-3-one (8q)** (%): mp >225 °C;  $^1\text{H NMR}$ ,  $\text{DMSO-}d_6$ ,  $\delta$  7.08 (d,  $J$  = 9 Hz, 1H), 7.60 (d,  $J$  = 8 Hz, 1H), 7.87 (d,  $J$  = 8 Hz, 1H), 8.07 (d,  $J$  = 9 Hz, 1H), 8.33 (m, 1H), 13.85 (s, 1H).

**6-(2,4-Difluorobenzenesulfonyl)-2H-pyridazin-3-one (8r)** (41%): mp 186–188 °C;  $^1\text{H NMR}$ ,  $\text{DMSO-}d_6$ ,  $\delta$  7.09 (d,  $J$  = 8 Hz, 1H), 7.72 (d,  $J$  = 8 Hz, 1H), 7.93 (m, 3H), 13.84 (s, 1H).

**6-(2-Chloro-4-fluorobenzenesulfonyl)-2H-pyridazin-3-one (8s)** (74%): mp 205–208 °C;  $^1\text{H NMR}$ ,  $\text{DMSO-}d_6$ ,  $\delta$  7.13 (d,  $J$  = 9 Hz, 1H), 7.60 (dd,  $J$  = 8 Hz, 2 Hz, 1H), 7.87 (dd,  $J$  = 8 Hz, 2 Hz, 1H), 8.02 (d,  $J$  = 9 Hz, 1H), 8.33 (m, 1H), 13.82 (s, 1H).

**6-(4-Trifluoromethylbenzenesulfonyl)-2H-pyridazin-3-one (8v)** (47%): mp 214–222 °C;  $^1\text{H NMR}$ ,  $\text{DMSO-}d_6$ , 7.02 (d,  $J$  = 11 Hz, 1H), 7.55–7.65 (m, 4H), 7.75 (m, 1H), 13.90 (s, 1H).

**6-( $\alpha$ -Naphthylmethylbenzenesulfonyl)-2H-pyridazin-3-one (8w)** (16%): mp 225–226 °C;  $^1\text{H NMR}$ ,  $\text{DMSO-}d_6$ ,  $\delta$  7.05 (d,  $J$  = 9 Hz, 1H), 7.67–7.84 (m, 3H), 8.02 (d,  $J$  = 9 Hz, 1H), 8.17 (dd,  $J$  = 8 Hz, 1H), 8.40–8.51 (m, 3H), 13.76 (s, 1H).

**6-( $\beta$ -Naphthylmethylbenzenesulfonyl)-2H-pyridazin-3-one (8x)** (49%): mp 232–233 °C;  $^1\text{H NMR}$ ,  $\text{DMSO-}d_6$ ,  $\delta$  7.01 (d,  $J$  = 9 Hz, 1H), 7.80 (d,  $J$  = 9 Hz, 1H), 7.89 (s, 1H), 8.35 (s, 2H), 13.76 (s, 1H).

**6-(2-Fluorobenzenesulfonyl)-2H-pyridazin-3-one (8f).**  
**Step 1.** To a clear solution of 4-fluorothiophenol (20 mmol, 2.58 g) and *t*-BuOK (2.24 20 mmol) in DMF (10 mL) was added 3-chloro-6-methoxy-pyridazine (20 mmol, 2.85 g) and the mixture stirred at room temperature for 1 h. The reaction mixture was quenched with  $\text{H}_2\text{O}$  (30 mL) and extracted with EtOAc (50 mL). The EtOAc layer was collected and washed with  $\text{H}_2\text{O}$ , and the organic portion was collected, dried, and filtered, and the filtrate was evaporated to obtain crude 3-(2-fluorophenylsulfanyl)-6-methoxy-pyridazine (85%): mp 58–62 °C.

**Step 2.** A mixture of 3-(2-fluorophenylsulfanyl)-6-methoxy-pyridazine (500 mg, 1.9 mmol), MCPBA (1.04 g, 7.3 mmol), and  $\text{CH}_2\text{Cl}_2$  (10 mL) was prepared and stirred at room temperature for 2 h. The reaction mixture was diluted with  $\text{CH}_2\text{Cl}_2$  and the  $\text{CH}_2\text{Cl}_2$  layer was washed with saturated sodium bicarbonate (10 mL) and then with  $\text{H}_2\text{O}$ . The  $\text{CH}_2\text{Cl}_2$  layer was collected, dried, and filtered, and the filtrate was evaporated to dryness. The residue was purified by silica gel chromatography (3:1 EtOAc/hexane as eluent) to obtain 3-(2-fluorobenzenesulfonyl)-6-methoxy-pyridazine as a white solid (51%):  $^1\text{H NMR}$ ,  $\text{DMSO-}d_6$ ,  $\delta$  4.19 (s, 3H), 7.13 (d,  $J$  = 8 Hz, 1H), 7.21 (d,  $J$  = 8 Hz, 1H), 8.13 (m, 4H).

**Step 3.** A mixture of 3-(2-fluorobenzenesulfonyl)-6-methoxy-pyridazine (200 mg, 0.84 mmol) and concentrated HCl (2 mL) was prepared and refluxed for 1h. The reaction mixture was cooled and diluted with  $\text{H}_2\text{O}$  (20 mL). Sufficient 40% aqueous NaOH was then added to adjust the pH of the mixture to 3 and the mixture was extracted with EtOAc. The EtOAc extracts were collected, combined, dried, and filtered. The filtrate was evaporated to obtain **8f** as a white solid (80 mg, 45%): mp 189–191 °C;  $^1\text{H NMR}$ ,  $\text{DMSO-}d_6$ , 7.06 (d,  $J$  = 8 Hz, 1H), 7.23 (m, 1H), 7.3 (m, 1H), 7.89 (d,  $J$  = 8 Hz, 1H), 8.02 (m, 2H) and 13.82 (s, 1H).

**6-(Biphenyl-2-sulfonyl)-2H-pyridazin-3-one (8j).** **Step 1. 6-(Biphenyl-2-sulfonyl)-6-methoxy-pyridazine.** A mixture of benzenesulfonic acid (157 mg, 1.2 mmol), 6-(4-bromobenzenesulfonyl)-6-methoxy-pyridazine (247 mg, 0.8 mmol),  $K_2CO_3$  (207 mg),  $Pd[P(Ph)_3]_4$  (87 mg), toluene (4 mL), EtOH (2 mL), and  $H_2O$  (1.5 mL) was prepared and refluxed for 4 h. The mixture was cooled and  $H_2O$  was added (10 mL). The mixture was then filtered, and the resulting filtrate was extracted with EtOAc (20 mL). The EtOAc extract was washed with  $H_2O$  and the EtOAc portion was collected, dried, and filtered. The filtrate was collected and evaporated to dryness to afford the title product of step 1.

**Step 2.** The product of step 1 was treated with concentrated HCl according to step 3 of example 8d to obtain the title compound (40%): mp 207–208 °C;  $^1H$  NMR, DMSO- $d_6$ ,  $\delta$  7.25 (d,  $J$  = 9 Hz, 1H), 7.05 (m, 4H), 7.27–7.41 (b, 5H), 8.28 (d,  $J$  = 9 Hz, 1H), 13.57 (s, 1H).

**6-(4-Bromo-2-fluorobenzenesulfonyl)-2H-pyridazin-3-one (8t).** **Step 1.** A mixture of 2-fluoro-4-bromothiophenol (300 mg, 1.6 mmol), 3,6-dichloro-pyridazine (149 mg, 1.0 mmol),  $K_2CO_3$  (400 mg), and acetone (6 mL) was prepared and refluxed for 2 h. The acetone from the mixture was evaporated and the resulting residue was dissolved in a solution of methanol (3 mL) and sodium metal (166 mg, 7.2 mmol). The resulting solution was refluxed for 1 h. Evaporation of methanol afforded 3-(4-bromo-2-fluorophenylsulfanyl)-6-methoxy-pyridazine, which was not isolated but was immediately used in step 2.

**Step 2.** The product of step 1 (400 mg, 1.3 mmol) was dissolved in  $CHCl_3$  (10 mL), and MCPBA (770 mg, 4.5 mmol) was added to the resulting solution. The reaction mixture was stirred overnight at room temperature. The solvent was evaporated and the resulting residue was purified by silica gel chromatography (90% hexane/10% EtOAc as eluent) to obtain 3-(4-bromo-2-fluorobenzenesulfonyl)-6-methoxy-pyridazine (60%).

**Step 3.** A mixture of 3-(4-bromo-2-fluorobenzenesulfonyl)-6-methoxy-pyridazine (260 mg), dioxane (5 mL), and concentrated HCl (1 mL) was prepared and refluxed for 2 h. The reaction mixture was then evaporated to dryness. The resulting residue was triturated with  $H_2O$  and the precipitated solid was collected and air-dried to obtain the title compound (90%): mp > 220 °C;  $^1H$  NMR, DMSO- $d_6$ ,  $\delta$  7.05 (d,  $J$  = 8 Hz, 1H), 7.7 (d,  $J$  = 8 Hz, 1H), 7.9 (m, 3H), 13.8 (s, 1H).

**6-(3-Trifluoromethylbenzenesulfonyl)-2H-pyridazin-3-one (8u).** A mixture of 3,6-dichloropyridazine (30 mmol, 4.4 g), 3-trifluoromethylphenylsulfonic acid sodium salt (30 mmol, 6.9 g), 2-propanol (30 mL), and  $H_2O$  (1 mL) was prepared and refluxed for 18 h. The reaction mixture was then cooled and diluted with  $H_2O$  (100 mL), and the precipitated solid was collected. The solid was triturated with *n*-propanol and the solid was collected to obtain the title compound (25%): mp > 230 °C;  $^1H$  NMR, DMSO- $d_6$ ,  $\delta$  7.10 (d,  $J$  = 11 Hz, 1H), 8.01 (d,  $J$  = 11 Hz, 1H), 8.10 (d,  $J$  = 8 Hz, 2H), 8.21 (d,  $J$  = 8 Hz, 2H), 13.90 (s, 1H).

**8-Phenylsulfonylphthalazin-2H-3-one (8y).** **Step 1.** To a solution of sodium metal (15 mmol, 0.345 g) in MeOH (10 mL) was added thiophenol (12.5 mmol, 1.38 g, 1.3 mL) and stirred for 30 min. The solution was evaporated to dryness and to the solid residue was added toluene (20 mL), followed by 1,4-dichlorophthalazine (10.0 mmol, 1.99 g), and the mixture refluxed for 1.5 h. Excess toluene was evaporated and the residue was chromatographed over silica gel. Elution with hexane/EtOAc (1:1) and evaporation of solvents gave 3-chloro-8-phenylsulfonylphthalazine (23%, 590 mg): mp 173–177 °C. This was used in step 2.

**Step 2.** A mixture of 3-chloro-8-phenylsulfonylphthalazine (2.32 mmol), MCPBA (4.1 mmol, 1.07 g), and  $CHCl_3$  (30 mL) was stirred at room temperature for 3 h. The reaction mixture was diluted with  $CHCl_3$  and washed with saturated aqueous  $Na_2CO_3$ , the organic portion was dried and evaporated to dryness, and the residue was crystallized from IPO to obtain 8y (47%, 310 mg): mp > 225 °C;  $^1H$  NMR, DMSO- $d_6$ ,  $\delta$  7.72 (d,  $J$  = 8 Hz, 2H), 7.81 (d,  $J$  = 8 Hz, 1H), 8.00 (d,  $J$  = 8 Hz,

1H), 8.08 (m, 3H), 8.34 (d,  $J$  = 8 Hz, 1H), 8.52 (d,  $J$  = 8 Hz, 1H), 13.31 (s, 1H).

The following, 15a–k, were prepared according to the method of Kukulja et al.<sup>24</sup> using the requisite benzyl halides.

**6-(2-Cl-phenylmethanesulfonyl)-2H-pyridazin-3-one (15a)** (63%): mp 175–176 °C;  $^1H$  NMR, DMSO- $d_6$ ,  $\delta$  4.98 (s, 2H), 7.03 (d,  $J$  = 9.9 Hz, 1H), 7.61–7.65 (m, 4H), 7.75 (m, 1H), 13.89 (s, 1H).

**6-(2-F-phenylmethanesulfonyl)-2H-pyridazin-3-one (15b)** (72%): mp 181–182 °C;  $^1H$  NMR, DMSO- $d_6$ ,  $\delta$  4.94 (s, 2H), 7.08 (d,  $J$  = 9.9 Hz, 1H), 7.25–7.43 (m, 2H), 7.46–7.54 (m, 2H), 7.75 (d,  $J$  = 9.9 Hz, 1H), 13.82 (s, 1H).

**6-(2-CF<sub>3</sub>-phenylmethanesulfonyl)-2H-pyridazin-3-one (15c)** (54%): mp 190–191 °C;  $^1H$  NMR, DMSO- $d_6$ ,  $\delta$  4.99 (s, 2H), 7.03 (d,  $J$  = 9.9 Hz, 1H), 7.55–7.65 (m, 4H), 7.75 (m, 1H), 13.89 (s, 1H).

**6-(3-CF<sub>3</sub>-phenylmethanesulfonyl)-2H-pyridazin-3-one (15d)** (64%): mp 227–228 °C;  $^1H$  NMR, DMSO- $d_6$ ,  $\delta$  4.92 (s, 2H), 7.02 (d,  $J$  = 10 Hz, 1H), 7.42 (m, 2H), 7.48–7.59 (m, 2H), 7.75 (d,  $J$  = 10 Hz, 1H), 13.89 (s, 1H).

**6-(2,3-Cl<sub>2</sub>-phenylmethanesulfonyl)-2H-pyridazin-3-one (15e)** (72%): mp > 230 °C;  $^1H$  NMR, DMSO- $d_6$ ,  $\delta$  5.01 (s, 2H), 7.01 (d,  $J$  = 9.9 Hz, 1H), 7.42–7.47 (m, 2H), 7.62–7.71 (m, 1H), 7.78 (d,  $J$  = 9.9 Hz, 1H), 13.83 (s, 1H).

**6-(2,6-Cl<sub>2</sub>-phenylmethanesulfonyl)-2H-pyridazin-3-one (15f)** (76%):  $^1H$  NMR, DMSO- $d_6$ ,  $\delta$  4.99 (s, 2H), 7.03 (d,  $J$  = 9.9 Hz, 1H), 7.62–7.71 (m, 3H), 7.78 (d,  $J$  = 9.9 Hz, 1H), 13.89 (s, 1H).

**6-(2,3-F<sub>2</sub>-phenylmethanesulfonyl)-2H-pyridazin-3-one (15g)** (47%):  $^1H$  NMR, DMSO- $d_6$ ,  $\delta$  4.94 (s, 2H), 7.01 (d,  $J$  = 10 Hz, 1H), 7.42 (m, 1H), 7.44–7.54 (m, 2H), 7.72 (d,  $J$  = 10 Hz, 1H), 13.84 (s, 1H).

**6-(2F,4Br-phenylmethanesulfonyl)-2H-pyridazin-3-one (15h)** (53%):  $^1H$  NMR, DMSO- $d_6$ ,  $\delta$  4.98 (s, 2H), 7.03 (d,  $J$  = 9.9 Hz, 1H), 7.38 (m, 1H), 7.62–7.71 (m, 2H), 7.78 (d,  $J$  = 9.9 Hz, 1H).

**6-(2Cl,6F-phenylmethanesulfonyl)-2H-pyridazin-3-one (15i)** (68%): mp > 230 °C;  $^1H$  NMR, DMSO- $d_6$ ,  $\delta$  4.99 (s, 2H), 7.03 (d,  $J$  = 9.9 Hz, 1H), 7.42 (m, 1H), 7.62–7.71 (m, 2H), 7.78 (d,  $J$  = 9.9 Hz, 1H), 13.89 (s, 1H).

**6-(2F,3-Cl-phenylmethanesulfonyl)-2H-pyridazin-3-one (15j)** (49%):  $^1H$  NMR, DMSO- $d_6$ ,  $\delta$  4.99 (s, 2H), 7.03 (d,  $J$  = 9.9 Hz, 1H), 7.62–7.71 (m, 3H), 7.78 (d,  $J$  = 9.9 Hz, 1H), 13.89 (s, 1H).

**6-(2F,3-CF<sub>3</sub>-phenylmethanesulfonyl)-2H-pyridazin-3-one (15k)** (47%): mp 188–191 °C;  $^1H$  NMR, DMSO- $d_6$ ,  $\delta$  4.99 (s, 2H), 7.03 (d,  $J$  = 9.9 Hz, 1H), 7.62–7.71 (m, 3H), 7.78 (d,  $J$  = 9.9 Hz, 1H), 13.89 (s, 1H).

**6-(Indole-2-sulfonyl)-2H-pyridazin-3-one (19a).** **Method 1. Step 1.** To a solution of 2-mercaptoindole (6.7 mmol, 1.0 g) in acetone (20 mL) was added 3-chloro-6-methoxy-pyridazine (144 mmol, 1.52 g) and  $K_2CO_3$  (70 mmol, 0.98 g), and the mixture was refluxed for 2 h. Excess acetone was removed and the residue was partitioned between  $CHCl_3$  and  $H_2O$ . The  $CHCl_3$  layer was collected, dried, and filtered, and the filtrate was evaporated to a residue, which was purified by silica gel chromatography (eluent, hexanes–EtOAc/4:1) to obtain 6-(indole-2-sulfonyl)-3-methoxy-pyridazine (31%, 534 mg).

**Step 2.** To a solution of 6-(indole-2-sulfonyl)-3-methoxy-pyridazine (1.9 mmol, 488 mg) in  $CHCl_3$  (20 mL) was added MCPBA (4.1 mmol, 1.0 g), and the reaction stirred overnight at room temperature. The reaction was filtered and the filtrate was washed with saturated sodium bicarbonate solution (20 mL) and  $H_2O$  (20 mL). The  $CHCl_3$  layer was collected, filtered, and dried and the filtrate was evaporated to a residue, which was purified by silica gel chromatography (eluent, hexanes–EtOAc/3:1) to obtain the desired product, 6-(indole-2-sulfonyl)-3-methoxy-pyridazine (33%, 180 mg).

**Step 3.** A mixture of 6-(indole-2-sulfonyl)-3-methoxy-pyridazine (0.58 mmol, 290 mg), concentrated HCl (0.5 mL), and dioxane (3 mL) was heated at 100 °C for 2 h. The reaction was cooled and evaporated to dryness.  $H_2O$  (10 mL) was added to the residue, and the resulting solid, 6-(indole-2-sulfonyl)-

2*H*-pyridazin-3-one (19a), was collected (83%, 133 mg): mp 248–249 °C; <sup>1</sup>H NMR, DMSO-*d*<sub>6</sub>, δ 7.3 (d, *J* = 8 Hz, 1H), 7.40 (m, 1H), 7.60 (m, 2H), 7.80 (m, 2H), 8.0 (d, *J* = 8 Hz, 1H), 13.84 (s, 1H).

**6-(Indole-2-sulfonyl)-2*H*-pyridazin-3-one (19a). Method 2. Step 1.** *t*-BuLi (2.5 M in hexane, 6.5 mmol, 4.3 mL) was added dropwise over 15 min to a solution of *N*-sulfonylphenyl indole (2.88 mmol, 520 mg) in THF (8 mL) cooled to –78 °C. To this was added 3-fluorosulfonyl-6-methoxy-pyridazine (5.2 mmol, 1.0 g) and stirred for 30 min. The reaction was allowed to come to room temperature overnight and then quenched with EtOAc (20 mL) and H<sub>2</sub>O (10 mL). The organic portion was collected, dried, and filtered, and the filtrate was evaporated to dryness to obtain a crude product, which was purified by silica gel chromatography (eluent, hexanes–EtOAc, 7:1) to obtain 3-methoxy-6-(*N*-phenylsulfonylindole-2-sulfonyl)pyridazine (39%, 867 mg).

**Step 2.** To a solution of sodium metal (18.6 mmol, 428 mg) dissolved in MeOH (8 mL) was added a solution of 3-methoxy-6-(*N*-phenylsulfonylindole-2-sulfonyl)pyridazine (1.86 mmol, 850 mg) and the reaction was stirred for 10 min. The reaction was quenched with H<sub>2</sub>O (10 mL) and CHCl<sub>3</sub> (25 mL). The CHCl<sub>3</sub> layer was collected, dried, and filtered, and the filtrate was evaporated to obtain 6-(indole-2-sulfonyl)-3-methoxy-pyridazine (82%, 440 mg).

**Step 3.** A mixture of 6-(indole-2-sulfonyl)-3-methoxy-pyridazine (1.03 mmol, 300 mg), concentrated HCl (1 mL), and dioxane (6 mL) was heated at 100 °C for 2 h. The reaction was cooled and evaporated to dryness. H<sub>2</sub>O (10 mL) was added to the residue, and the resulting solid was triturated with MeOH (2 mL) to yield 6-(indole-2-sulfonyl)-2*H*-pyridazin-3-one, **19a** (37%).

**6-(5-Chloroindole-2-sulfonyl)-2*H*-pyridazin-3-one (19b)** was prepared according to the method for **19a**, starting from 5-chloro-*N*-*p*-tolylsulfonyl indole (64%): mp >250 °C; <sup>1</sup>H NMR, DMSO-*d*<sub>6</sub>, δ 7.06 (d, 1H, *J* = 10 Hz), 7.29 (s, 1H), 7.32 (d, 1H, *J* = 8 Hz), 7.46 (d, 1H, *J* = 8 Hz), 7.77 (s, 1H), 7.92 (d, 1H, *J* = 10 Hz), 12.74 (s, 1H), 13.80 (s, 1H).

The following were prepared according to procedures for **19a**, method 2, starting from appropriate starting materials and reagents.

**6-(6-Chloroindole-2-sulfonyl)-2*H*-pyridazin-3-one (19c)** was prepared according to the method for **19a**, starting from 6-chloro-*N*-*p*-tolylsulfonylindole (95%): mp >250 °C; <sup>1</sup>H NMR, DMSO-*d*<sub>6</sub>, δ 7.05 (d, *J* = 10 Hz, 1H), 7.15 (d, *J* = 8 Hz, 1H), 7.34 (s, 1H), 7.46 (s, 1H), 7.72 (d, *J* = 8 Hz, 1H), 7.92 (d, *J* = 10 Hz, 1H), 12.69 (s, 1H), 13.80 (s, 1H).

**6-(7-Chloroindole-2-sulfonyl)-2*H*-pyridazin-3-one (19d)** was prepared according to the method for **19a** starting from 7-chloro-*N*-*p*-tolylsulfonyl indole (76%): mp 248–250 °C; <sup>1</sup>H NMR, DMSO-*d*<sub>6</sub>, δ 7.07–7.16 (m, 2H), 7.41–7.45 (m, 2H), 7.69 (d, *J* = 8 Hz, 1H), 8.01 (d, *J* = 10 Hz, 1H), 12.83 (s, 1H), 13.74 (s, 1H).

**6-(6-Fluoroindole-2-sulfonyl)-2*H*-pyridazin-3-one (19e)** was prepared according to the method for **19a**, starting from 6-fluoro-*N*-*p*-tolylsulfonylindole (90%): mp >250 °C; <sup>1</sup>H NMR, DMSO-*d*<sub>6</sub>, δ 7.03 (m, 2H), 7.17 (d, *J* = 8 Hz, 1H), 7.34 (s, 1H), 7.74 (d, *J* = 8 Hz, 1H), 7.92 (d, *J* = 10 Hz, 1H), 12.63 (s, 1H), 13.78 (s, 1H).

**6-(5,6-Methylenedioxyindole-2-sulfonyl)-2*H*-pyridazin-3-one (19f)** was prepared according to the method for **19a**, starting from 5,6-methylenedioxy-*N*-*p*-tolylsulfonyl indole (67%): mp 250 °C; <sup>1</sup>H NMR, DMSO-*d*<sub>6</sub>, δ 5.99 (s, 2H), 6.86 (s, 1H), 7.04 (d, *J* = 10 Hz, 1H), 7.08 (s, 1H), 7.14 (s, 1H), 7.88 (d, *J* = 10 Hz, 1H), 12.34 (s, 1H), 13.71 (s, 1H).

**6-(5,7-Dichloroindole-2-sulfonyl)-2*H*-pyridazin-3-one (19g)** was prepared according to the method for **19a** starting from 5,7-dichloro-*N*-*p*-tolylsulfonyl indole (80%): mp >250 °C; <sup>1</sup>H NMR, DMSO-*d*<sub>6</sub>, δ 7.15 (d, *J* = 10 Hz, 1H), 7.42 (s, 1H), 7.56 (s, 1H), 7.80 (s, 1H), 8.20 (d, *J* = 10 Hz, 1H), 13.15 (s, 1H), 13.78 (s, 1H).

**6-(3-Methylbenzofuran-2-sulfonyl)-2*H*-pyridazin-3-one (19j). Step 1.** A solution of 2-bromo-3-methylbenzofuran (1.34 mmol, 283 mg) in THF (5 mL) was cooled to –78 °C and

to it was added *n*-BuLi (2.5 M in hexane, 1.47 mmol, 0.6 mL) dropwise. The reaction was stirred for 30 min and 3-fluoro-sulfonyl-6-methoxy-pyridazine (1.34 mmol, 257 mg) was added to it. The reaction was allowed to come to room temperature overnight and was diluted with EtOAc (20 mL) and H<sub>2</sub>O (10 mL). The organic portion was collected, dried, and filtered, and the filtrate was evaporated to dryness to obtain a brown oil, 6-(3-methylbenzofuran-2-sulfonyl)-3-methoxy-pyridazine (52%, 212 mg).

**Step 2.** A mixture of 6-(3-methylbenzofuran-2-sulfonyl)-3-methoxy-pyridazine (0.73 mmol, 212 mg), concentrated HCl (2 mL), and dioxane (3 mL) was heated at 100 °C for 2 h. The reaction was cooled and evaporated to dryness to obtain a crude product, which was purified by silica gel chromatography (eluent, EtOAc–hexanes, 1:1), to obtain 6-(3-methylbenzofuran-2-sulfonyl)-2*H*-pyridazin-3-one (31%, 65 mg): mp 182–183 °C; <sup>1</sup>H NMR, DMSO-*d*<sub>6</sub>, δ 2.6 (s, 3H), 7.1 (d, *J* = 8 Hz, 1H), 7.4 (m, 1H), 7.55 (m, 2H), 7.75 (m, 1H), 8.0 (d, *J* = 8 Hz, 1H), 13.86 (s, 1H).

**6-(5-Chloro-3-methylbenzofuran-2-sulfonyl)-2*H*-pyridazin-3-one (19m). Method 1. Step 1.** *n*-Butyllithium (2.5 M in hexane, 0.09 mol, 33 mL) was added dropwise over 15 min to a solution of 5-chloro-3-methylbenzofuran<sup>41</sup> (0.09 mol, 15g) in THF (160 mL), cooled to –78 °C. To this was added sulfur powder (0.09 mol, 2.7 g) and the mixture stirred for 10 min. The reaction was allowed to come to room temperature and then quenched with Et<sub>2</sub>O (200 mL) and H<sub>2</sub>O (500 mL). Sufficient 10% HCl was added to adjust the pH to 7. The ether layer was collected, dried, and filtered, and the filtrate was evaporated to dryness to obtain a pale yellow solid, 5-chloro-2-mercapto-3-methylbenzofuran (90%, 15.1 g).

**Step 2.** To a solution containing 5-chloro-2-mercapto-3-methylbenzofuran (10 mmol, 1.98 g) and 3-chloro-6-methoxy-pyridazine (10 mmol, 1.44 g) in DMF (10 mL) was added K<sub>2</sub>CO<sub>3</sub> (20 mmol, 2.76 g), and the reaction was stirred at room temperature for 3 h. The reaction was quenched with H<sub>2</sub>O (200 mL), the precipitated yellow solid was collected, and the solid was purified by silica gel chromatography (eluent, hexanes–EtOAc, 9:1) to obtain 6-(5-chloro-3-methylbenzofuran-2-sulfonyl)-3-methoxy-pyridazine (93%, 2.87 g): mp 131–134 °C.

**Step 3.** A mixture of 6-(5-chloro-3-methylbenzofuran-2-sulfonyl)-3-methoxy-pyridazine (1.6 mmol, 500 mg), concentrated HCl (1 mL), and dioxane (5 mL) was heated at 100 °C for 2 h. The reaction was cooled and evaporated to dryness. H<sub>2</sub>O (10 mL) was added to the residue, and the resulting white precipitate was collected and crystallized from EtOH to obtain the desired product, 6-(5-chloro-3-methylbenzofuran-2-sulfonyl)-2*H*-pyridazin-3-one (73%, 113 mg).

**Step 4.** To a mixture of 6-(5-chloro-3-methylbenzofuran-2-sulfonyl)-2*H*-pyridazin-3-one and AcOH (30 mL) was added peracetic acid (33 mmol, 7.8 mL). The reaction was allowed to stir overnight and the precipitated solid was collected and washed with H<sub>2</sub>O. The solid was air-dried and crystallized from MeOH to give 6-(5-chloro-3-methylbenzofuran-2-sulfonyl)-2*H*-pyridazin-3-one, (37%, 1.81 g): mp 247–248 °C; <sup>1</sup>H NMR, DMSO-*d*<sub>6</sub>, δ 2.6 (s, 3H), 7.1 (d, *J* = 8 Hz, 1H), 7.55 (m, 2H), 7.8 (s, 1H), 8.0 (d, *J* = 8 Hz, 1H), 13.84 (s, 1H).

**6-(5-Chloro-3-methylbenzofuran-2-sulfonyl)-2*H*-pyridazin-3-one (19m). Method 2. Step 1.** *n*-BuLi (2.5 M in hexane, 1.2 mmol, 0.48 mL) was added dropwise over 15 min to a solution of 5-chloro-3-methylbenzofuran (1.92 mmol, 320 mg) in THF (6 mL) cooled to –78 °C. To this was added 3-fluorosulfonyl-6-methoxy-pyridazine (1.92 mmol, 369 mg) and the mixture stirred for 30 min. The reaction was allowed to come to room temperature overnight and then quenched with EtOAc (20 mL) and H<sub>2</sub>O (10 mL). The organic portion was collected, dried, and filtered, and the filtrate was evaporated to dryness to obtain a crude product, which was purified by silica gel chromatography (eluent, hexanes–EtOAc, 3:2) to obtain 6-(5-chloro-3-methylbenzofuran-2-sulfonyl)-3-methoxy-pyridazine (22%, 166 mg).

**Step 2.** A mixture of 6-(5-chloro-3-methylbenzofuran-2-sulfonyl)-3-methoxy-pyridazine (0.5 mmol, 162 mg), concentrated HCl (1 mL), and dioxane (3 mL) was heated at 100 °C

for 2 h. The reaction was cooled and evaporated to dryness. H<sub>2</sub>O (10 mL) was added to the residue, and the resulting yellow precipitate was collected and crystallized from EtOH to obtain 6-(5-chloro-3-methylbenzofuran-2-sulfonyl)-2H-pyridazin-3-one (73%, 113 mg).

**6-(5-Chloro-3-methylbenzofuran-2-sulfonyl)-2H-pyridazin-3-one (19m).** Method 3. Step 1. *n*-Butyllithium (2.5 M in hexane, 33 mmol, 13.2 mL) was added dropwise over 15 min to a solution of 5-chloro-3-methylbenzofuran (30.0 mmol, 5 g) in THF (30 mL) cooled to between -50 and -35 °C. This was transferred into a cold-jacketed addition funnel and added dropwise to a solution of 3-fluorosulfonyl-6-methoxyppyridazine (30 mmol, 5.76 g) in THF (30 mL) over 10 min. The reaction was allowed to come to room temperature, excess solvents were removed, and the residue was quenched with H<sub>2</sub>O (500 mL). The granulated product was filtered and air-dried to obtain 6-(5-chloro-3-methylbenzofuran-2-sulfonyl)-3-methoxyppyridazine (75%, 7.62 g).

**Step 2.** A mixture of 6-(5-chloro-3-methylbenzofuran-2-sulfonyl)-3-methoxyppyridazine (22.2 mmol, 7.5 g), concentrated HCl (5 mL), and dioxane (50 mL) was heated at 100 °C for 2 h. The reaction was cooled and evaporated to dryness. H<sub>2</sub>O (20 mL) was added to the residue, the resulting precipitate was collected and crystallized from EtOH to obtain 6-(5-chloro-3-methylbenzofuran-2-sulfonyl)-2H-pyridazin-2H-pyridazin-3-one, **19n** (89%, 6.42 g).

**6-(Benzofuran-2-sulfonyl)-2H-pyridazin-3-one (19h)** was prepared according to example **19m**, method 2, but starting from benzofuran (10%): mp 210–211 °C; <sup>1</sup>H NMR, DMSO-*d*<sub>6</sub>, δ 7.1 (d, *J* = 8 Hz, 1H), 7.35 (m, 1H), 7.56 (m, 2H), 7.82 (m, 2H), 8.0 (d, *J* = 8 Hz, 1H), 13.9 (s, 1H).

**6-(5-Chlorobenzofuran-2-sulfonyl)-2H-pyridazin-3-one (19i)** was prepared according to example **19m**, method 3, but starting from 5-chlorobenzofuran (68%): mp 246–247 °C; <sup>1</sup>H NMR, DMSO-*d*<sub>6</sub>, δ 7.15 (d, *J* = 8 Hz, 1H), 7.50 (m, 2H), 7.82 (d, *J* = 4 Hz, 2H), 8.0 (d, *J* = 8 Hz, 1H), 13.82 (s, 1H).

**6-(5-Methoxybenzofuran-2-sulfonyl)-2H-pyridazin-3-one (19k)** was prepared according to example **19m**, method 3, but starting from 5-methoxybenzofuran (28%): mp 222–223 °C; <sup>1</sup>H NMR, DMSO-*d*<sub>6</sub>, δ 3.8 (s, 3H), 7.05 (d, *J* = 8 Hz, 1H), 7.15 (dd, 1H, *J* = 2, 6 Hz), 7.5 (d, *J* = 6 Hz), 7.5 (s, 1H), 8.0 (d, *J* = 8 Hz, 1H), 13.82 (s, 1H).

**6-(5,7-Dichlorobenzofuran-2-sulfonyl)-2H-pyridazin-3-one (19l)** was prepared according to example **19m**, method 3, but starting from 5,7-dichloro-benzofuran: mp 240–245 °C; <sup>1</sup>H NMR, DMSO-*d*<sub>6</sub>, δ 7.15 (d, *J* = 8 Hz, 1H), 7.65 (d, *J* = 2 Hz, 1H), 7.78 (d, *J* = 2 Hz, 1H), 7.85 (d, *J* = 2 Hz, 1H), 8.0 (d, *J* = 8 Hz, 1H), 13.82 (s, 1H).

**6-(5-Fluoro-3-methylbenzofuran-2-sulfonyl)-2H-pyridazin-3-one (19o).** Step 1. Chloroacetic acid (99.3 mmol, 9.4 g) was added to a suspension of 5-fluoro-2-hydroxyacetophenone (33.1 mmol, 5.1 g) in H<sub>2</sub>O (60 mL) containing NaOH (165.4 mmol, 6.6 g), and the mixture was refluxed for 3.5 h. The reaction was cooled to room temperature and poured into a separatory funnel, and the oily liquid at the bottom of the funnel was discarded. The aqueous top layer was collected, cooled to 0 °C, and acidified with concentrated HCl. The white precipitate was collected and air dried. The dry solid was crystallized from toluene to obtain 2-acetyl-4-fluorophenoxy acetic acid (57%, 4.3 g).

**Step 2.** Anhydrous NaOAc (139.3 mmol, 11.4 g) was added to a solution of the product of step 1 (3.24 mmol, 1.6 g) in acetic anhydride (70 mL) and heated for 3 h at 110 °C. After cooling, the reaction mixture was poured into H<sub>2</sub>O (100 mL) and stirred for 1 h. The aqueous solution was extracted with Et<sub>2</sub>O and washed with 3% aqueous KOH and H<sub>2</sub>O. The washed Et<sub>2</sub>O layer was collected, dried, and filtered, and the filtrate was evaporated to a brown residue, which was purified by silica gel chromatography (eluent, hexanes) to obtain 5-fluoro-3-methylbenzofuran (59%, 1.65 g).

**Step 3.** *n*-BuLi (2.5 M in hexane, 11 mmol, 4.83 mL) was added dropwise over 15 min to a solution of 5-fluoro-3-methylbenzofuran (11 mmol, 1.65 g) in THF (20 mL) cooled to -78 °C. To this was added 3-fluorosulfonyl-6-methoxyppyridazine (11 mmol, 2.11 g) and the mixture stirred for 30 min.

The reaction was allowed to come to room temperature overnight and then quenched with EtOAc (40 mL) and H<sub>2</sub>O (10 mL). The organic portion was collected, dried, and filtered, and the filtrate was evaporated to dryness to obtain a crude product, which was purified by silica gel chromatography (eluent, hexanes–EtOAc, 4:1) to obtain the desired product, 6-(5-fluoro-3-methylbenzofuran-2-sulfonyl)-3-methoxyppyridazine (22%, 781 mg).

**Step 4.** A mixture of 6-(5-fluoro-3-methylbenzofuran-2-sulfonyl)-3-methoxyppyridazine (2.4 mmol, 775 mg), concentrated HCl (1.5 mL), and dioxane (3 mL) was heated at 100 °C for 2 h. The reaction was cooled and evaporated to dryness. The dried residue was triturated with H<sub>2</sub>O (10 mL) and filtered to obtain 6-(5-fluoro-3-methylbenzofuran-2-sulfonyl)-2H-pyridazin-3-one (84%, 620 mg): mp 232–233 °C; <sup>1</sup>H NMR, DMSO-*d*<sub>6</sub>, δ 2.6 (s, 3H), 7.1 (d, *J* = 8 Hz, 1H), 7.3 (m, 1H), 7.5 (m, 1H), 7.6 (m, 1H), 8.0 (d, *J* = 8 Hz, 1H), 13.84 (s, 1H).

**6-(6-Chloro-3-methylbenzofuran-2-sulfonyl)-2H-pyridazin-3-one (19n)** was prepared according to the method for **19o**, starting from 4-chloro-2-hydroxyacetophenone (42%): mp >240 °C; <sup>1</sup>H NMR, DMSO-*d*<sub>6</sub>, δ 2.55 (s, 3H), 7.04 (d, *J* = 10 Hz, 1H), 7.45 (m, 1H), 7.79–7.95 (m, 2H), 7.8 (d, *J* = 10 Hz, 1H), 13.82 (s, 1H).

**6-(5-Trifluoromethyl-3-methylbenzofuran-2-sulfonyl)-2H-pyridazin-3-one (19p).** 5-Trifluoromethyl-3-methylbenzofuran was prepared following a procedure described by Larock et al.<sup>41</sup>

**Step 1.** A mixture of iodine (91.6 mmol, 23.2 g) and Na<sub>2</sub>CO<sub>3</sub> (91.6 mmol, 7.7 g) was added to a solution of α,α,α-trifluoro-*p*-cresol (83.3 mmol, 13.5 g) in THF (90 mL) and H<sub>2</sub>O (90 mL), and the reaction was allowed to stand at room temperature overnight. Sufficient thiourea (5% solution) was added to remove the excess I<sub>2</sub>, as indicated by the color change of the reaction from deep violet to brown. The reaction mixture was extracted with Et<sub>2</sub>O, the extract was dried and filtered, and the filtrate was concentrated to obtain a brown oil. This oil was distilled (bp, 105 °C at 44 mmHg) to obtain α,α,α-trifluoro-*o*-iodo-*p*-cresol (4.1 g, 75% pure, admixed with the starting α,α,α-trifluoro-*p*-cresol).

**Step 2.** To a mixture of the above 75% pure α,α,α-trifluoro-*o*-iodo-*p*-cresol (4.1 g, 17 mmol), K<sub>2</sub>CO<sub>3</sub> (7.7 g), and DMF (120 mL) was added allyl bromide (6.8 g). After 3 h the reaction mixture was poured into H<sub>2</sub>O (100 mL) and extracted with Et<sub>2</sub>O. The Et<sub>2</sub>O layer was collected, dried, and filtered, and the filtrate was concentrated to obtain a brown oil. This oil was distilled (bp 95–100 °C at 20 mmHg) to obtain a mixture (3:1) of allyl compounds.

**Step 3.** To a mixture of the above allyl compounds (3.9 g, 8.83 mmol of the desired), Na<sub>2</sub>CO<sub>3</sub> (22.1 mmol, 2.3 g), HCO<sub>2</sub>-Na (8.83 mmol, 0.81 g), *n*-BuNH<sub>4</sub>Cl (9.72 mmol, 2.7 g), and DMF (15 mL) was added Pd(OAc)<sub>2</sub> (0.44 mmol, 0.1 g). The reaction was heated to 80 °C and maintained at that temperature overnight. After bringing the reaction to room temperature, the mixture was filtered, the filtrate was dried and evaporated to give a crude product, which was purified by silica gel chromatography (eluent, hexanes) to obtain 3-methyl-5-trifluoromethylbenzofuran as a clear oil (44%, 780 mg).

**Step 4.** *n*-BuLi (2.5 M in hexane, 4.2 mmol, 1.7 mL) was added dropwise over 15 min to a solution of 3-methyl-5-trifluoromethylbenzofuran (3.82 mmol, 765 mg) in THF (10 mL) cooled to -78 °C. To this was added 3-fluorosulfonyl-6-methoxyppyridazine (3.82 mmol, 734 mg) and the mixture stirred for 30 min. The reaction was allowed to come to room temperature overnight and was then quenched with EtOAc (20 mL) and H<sub>2</sub>O (10 mL). The organic portion was collected, dried, and filtered, and the filtrate was evaporated to dryness to obtain a crude product, which was purified by silica gel chromatography (eluent, hexanes–EtOAc, 3:1) to obtain 6-(trifluoromethyl-3-methylbenzofuran-2-sulfonyl)-3-methoxyppyridazine (35%, 501 mg).

**Step 5.** A mixture of 6-(trifluoromethyl-3-methylbenzofuran-2-sulfonyl)-3-methoxyppyridazine (1.34 mmol, 500 mg), concentrated HCl (2 mL), and dioxane (4 mL) was heated at 100 °C

for 2 h. The reaction was cooled and evaporated to dryness. H<sub>2</sub>O (10 mL) was added to the residue, the resulting white solid was collected and air-dried to obtain the desired product, 6-(5-trifluoromethyl-3-methylbenzofuran-2-sulfonyl)-2H-pyridazin-3-one (56%, 270 mg): mp 244–245 °C; <sup>1</sup>H NMR, DMSO-*d*<sub>6</sub>, δ 2.6 (s, 3H), 7.1 (d, *J* = 8 Hz, 1H), 7.75 (d, *J* = 6 Hz, 1H), 7.85 (d, *J* = 6 Hz, 1H), 8.0 (d, *J* = 8 Hz, 1H), 8.2 (s, 1H), 13.89 (s, 1H).

**6-(3,5-Dimethylbenzofuran-2-sulfonyl)-2H-pyridazin-3-one (19q)** was prepared according to example 19m, method 3, but starting from 3,5-dimethylbenzofuran (68%): mp 246–247 °C; <sup>1</sup>H NMR, DMSO-*d*<sub>6</sub>, δ 2.6 (s, 3H), 2.8 (s, 3H), 7.1 (d, *J* = 8 Hz, 1H), 7.4 (m, 2H), 7.5 (s, 1H), 8.0 (d, *J* = 8 Hz, 1H), 13.78 (s, 1H).

**6-(5-Chloro-3-ethylbenzofuran-2-sulfonyl)-2H-pyridazin-3-one (19r).** **Step 1.** To a solution of 4-chlorophenol in THF (75 mL) and H<sub>2</sub>O (75 mL) was added a mixture of crushed I<sub>2</sub> (78.7 mmol, 20 g) and Na<sub>2</sub>CO<sub>3</sub> (78.7 mmol, 6.6 g). The reaction was stirred at room temperature overnight and then quenched with sufficient 5% sodium thiosulfate solution to turn the color of the reaction mixture from deep violet to light yellow and extracted with ether. The ether layer was collected and washed with H<sub>2</sub>O, the washed ether layer was dried and filtered, and the filtrate was evaporated to a crude product, which was purified by distillation to obtain 4-chloro-2-iodo phenol (7%, 1.3 g): mp 79–82 °C.

**Step 2.** To a mixture of 4-chloro-2-iodophenol (5.11 mmol, 1.3 g) in DMF (40 mL) and K<sub>2</sub>CO<sub>3</sub> (10 mmol, 1.4 g) was added crotyl bromide (10.2 mmol, 1.6 g) and the reaction was stirred at room temperature for 1 h. The reaction was quenched with H<sub>2</sub>O (100 mL) and extracted with EtOAc. The EtOAc layer was collected, dried, and filtered, and the filtrate was evaporated to obtain 4-chloro-2-iodo-*o*-crotylphenol (94%, 1.5 g).

**Step 3.** To a mixture of 4-chloro-2-iodo-*o*-crotylphenol (1.5 g, 4.86 mmol of the desired), Na<sub>2</sub>CO<sub>3</sub> (12.2 mmol, 1.3 g), HCO<sub>2</sub>-Na (4.86 mmol, 330 mg), *n*-BuNH<sub>4</sub>Cl (5.34 mmol, 1.5 g), and DMF (10 mL) was added Pd(OAc)<sub>2</sub> (0.24 mmol, 55 mg). The reaction was heated to 80 °C and maintained at that temperature overnight. After bringing the reaction to room temperature, the mixture was filtered, and the filtrate was dried and evaporated to give a crude product, which was purified by silica gel chromatography (eluent, hexanes) to obtain 5-chloro-3-ethylbenzofuran as a clear oil (60%, 530 mg).

**Step 4.** *n*-BuLi (2.5 M in hexane, 3.2 mmol, 1.3 mL) was added dropwise over 15 min to a solution of 5-chloro-3-ethylbenzofuran (2.88 mmol, 520 mg) in THF (8 mL) cooled to –78 °C. To this was added 3-fluorosulfonyl-6-methoxy-pyridazine (2.88 mmol, 553 mg), and the mixture stirred for 30 min. The reaction was allowed to come to room temperature overnight and then quenched with EtOAc (20 mL) and H<sub>2</sub>O (10 mL). The organic portion was collected, dried, and filtered, and the filtrate was evaporated to dryness to obtain a crude product, which was purified by silica gel chromatography (eluent, hexanes–EtOAc, 4:1) to obtain the desired product, 6-(5-chloro-3-ethylbenzofuran-2-sulfonyl)-3-methoxy-pyridazine (35%, 352 mg).

**Step 5.** A mixture of 6-(5-chloro-3-ethylbenzofuran-2-sulfonyl)-3-methoxy-pyridazine (1.04 mmol, 352 mg), concentrated HCl (1.5 mL), and dioxane (3 mL) was heated at 100 °C for 2 h. The reaction was cooled and evaporated to dryness. H<sub>2</sub>O (10 mL) was added to the residue, and the resulting solid, 6-(5-chloro-3-ethylbenzofuran-2-sulfonyl)-2H-pyridazin-3-one, was collected (46%, 155 mg): mp 209–210 °C; <sup>1</sup>H NMR, DMSO-*d*<sub>6</sub>, δ 1.1 (m, 3H), 2.45 (m, 2H), 7.2 (d, *J* = 8 Hz, 1H), 7.5 (m, 1H), 7.6 (m, 1H), 8.0 (d, *J* = 8 Hz, 1H) 13.82 (s, 1H).

**6-(5-Chloro-3-isopropylbenzofuran-2-sulfonyl)-2H-pyridazin-3-one (19s).** **Step 1.** *n*-BuLi (2.5 M in hexane, 4.04 mmol, 1.62 mL) was added dropwise over 15 min to a solution of 5-chloro-3-isopropylbenzofuran<sup>42</sup> (3.67 mmol, 715 mg) in THF (10 mL) cooled to –78 °C. To this was added 3-fluoro-sulfonyl-6-methoxy-pyridazine (3.67 mmol, 706 mg) and the mixture stirred for 30 min. The reaction was allowed to come to room temperature overnight and then quenched with EtOAc (20 mL) and H<sub>2</sub>O (10 mL). The organic portion was collected,

dried, and filtered and the filtrate was evaporated to dryness to obtain a crude product, which was purified by silica gel chromatography (eluent, hexanes–EtOAc, 4:1) to obtain the desired product, 6-(5-chloro-3-isopropylbenzofuran-2-sulfonyl)-3-methoxy-pyridazine (21%, 283 mg).

**Step 2.** A mixture of 6-(5-chloro-3-isopropylbenzofuran-2-sulfonyl)-3-methoxy-pyridazine (0.77 mmol, 283 mg), concentrated HCl (1.5 mL), and dioxane (3 mL) was heated at 100 °C for 2 h. The reaction was cooled and evaporated to dryness. The dried residue was triturated with H<sub>2</sub>O (10 mL) and filtered to obtain the desired product, 6-(5-chloro-3-isopropylbenzofuran-2-sulfonyl)-2H-pyridazin-3-one (79%, 215 mg): mp 211–212 °C; <sup>1</sup>H NMR, DMSO-*d*<sub>6</sub>, δ 1.4 (d, *J* = 6 Hz, 6H), 7.2 (d, *J* = 8 Hz, 1H), 7.5 (m, 1H), 7.6 (m, 1H), 8.0 (d, *J* = 8 Hz, 1H), 13.82 (s, 1H).

**6-(3-Phenylbenzofuran-2-sulfonyl)-2H-pyridazin-3-one (19t)** was prepared according to example 19m, method 3, starting from 3-phenylbenzofuran (65%): mp >220 °C; <sup>1</sup>H NMR, DMSO-*d*<sub>6</sub>, δ 7.02 (d, *J* = 10 Hz, 1H), 7.49–7.55 (m, 8H), 7.65 (m, 1H), 7.75 (d, *J* = 10 Hz, 1H), 13.82 (s, 1H).

**6-(3-[4-Fluorophenyl]benzofuran-2-methylsulfonyl)-2H-pyridazin-3-one (19u)** was prepared according to example 19m, method 3, (46%): mp >240 °C; <sup>1</sup>H NMR, DMSO-*d*<sub>6</sub>, δ 7.02 (d, *J* = 9.9 Hz, 1H), 7.35 (m, 2H), 7.43 (m, 1H), 7.56–7.65 (m, 4H), 7.77–7.82 (m, 2H). The starting material, 4-fluorophenylbenzofuran, was prepared as follows.

To an ice-cold solution of 3-coumaranone (10 mmol, 1.34 g) in Et<sub>2</sub>O (20 mL) was added 4-fluorophenylmagnesium bromide (2 M in Et<sub>2</sub>O, 20 mmol, 10 mL), and the reaction stirred for 3.5 h. The reaction was quenched with H<sub>2</sub>O (10 mL), the pH adjusted to 7 with sufficient 10% HCl, and reaction extracted with Et<sub>2</sub>O. The ether extract was collected, dried, filtered, and evaporated to dryness. The residue was purified by silica gel chromatography (eluent, hexanes) to obtain 4-fluorophenylbenzofuran.

**6-(5-Chloro-3-phenylbenzofuran-2-sulfonyl)-2H-pyridazin-3-one (19v)** was prepared according to example 19h, method 2, starting from 5-chloro-3-phenylbenzofuran: mp >240 °C; <sup>1</sup>H NMR, DMSO-*d*<sub>6</sub>, δ 7.02 (d, *J* = 9.9 Hz, 1H), 7.49–7.55 (m, 6H), 7.65 (m, 1H), 7.75 (d, *J* = 9.9 Hz, 1H), 7.86 (d, *J* = 8.7 Hz, 1H), 13.84 (s, 1H).

**6-(5-Chloro-3-methylbenzothioephene-2-sulfonyl)-2H-pyridazin-3-one (19y).** **Step 1.** *n*-BuLi (2.5 M in hexane, 2.1 mmol, 0.84 mL) was added dropwise over 15 min to a solution of 5-chloro-3-methylbenzothioephene<sup>43</sup> (1.91 mmol, 348 mg) in THF (6 mL) cooled to –78 °C. To this was added 3-fluoro-sulfonyl-6-methoxy-pyridazine (1.91 mmol, 366 mg) and the mixture stirred for 30 min. The reaction was allowed to come to room temperature overnight and then quenched with EtOAc (20 mL) and H<sub>2</sub>O (10 mL). The organic portion was collected, dried, and filtered, and the filtrate was evaporated to dryness to obtain a crude product, which was purified by silica gel chromatography (eluent, hexanes–EtOAc, 4:1) to obtain the desired product, 6-(5-chloro-3-methylbenzothioephene-2-sulfonyl)-3-methoxy-pyridazine (29%, 197 mg).

**Step 2.** A mixture of 6-(5-chloro-3-methylbenzothioephene-2-sulfonyl)-3-methoxy-pyridazine, (0.55 mmol, 197 mg), concentrated HCl (1 mL), and dioxane (3 mL) was heated at 100 °C for 2 h. The reaction was cooled and evaporated to dryness. H<sub>2</sub>O (10 mL) was added to the residue, and the resulting yellow precipitate, 6-(5-chloro-3-methylbenzothioephene-2-sulfonyl)-2H-pyridazin-3-one was collected (29%, 55 mg): mp 258–259 °C; <sup>1</sup>H NMR, DMSO-*d*<sub>6</sub>, δ 2.9 (s, 3H), 7.1 (d, *J* = 10 Hz, 1H), 7.55 (d, *J* = 9 Hz, 1H), 7.9 (d, *J* = 9 Hz, 1H), 7.95 (s, 1H), 8.0 (d, *J* = 10 Hz, 1H), 13.78 (s, 1H).

**6-(Benzothioephene-2-sulfonyl)-2H-pyridazin-3-one (19w)** was prepared according to the method for 19y, starting from benzothioephene (42%): mp 209–210 °C; <sup>1</sup>H NMR, DMSO-*d*<sub>6</sub>, δ 7.1 (d, *J* = 10 Hz, 1H), 7.5 (m, 2H), 8.0 (d, *J* = 10 Hz, 1H), 8.1 (m, 3H), 8.2 (s, 1H), 13.80 (s, 1H).

**6-(5-Methylbenzothioephene-2-sulfonyl)-2H-pyridazin-3-one (19x)** was prepared according to the method for 19y, starting from 5-methylbenzothioephene (62%): mp 240–242 °C; <sup>1</sup>H NMR, DMSO-*d*<sub>6</sub>, δ 2.4 (s, 3H), 7.1 (d, *J* = 10 Hz, 1H), 7.4

(d,  $J = 9$  Hz, 1H), 7.8 (d,  $J = 9$  Hz, 1H), 7.85 (s, 1H), 7.9 (d,  $J = 9$  Hz, 1H), 8.0 (d,  $J = 10$  Hz, 1H), 8.25 (s, 1H).

**6-(Benzothiazole-2-sulfonyl)-2H-pyridazin-3-one (19z)** was prepared according to the method of Kukulja et al.,<sup>24</sup> but starting from 2-chlorobenzothiazole and 3-mercapto-4-methoxy-pyridazine, **12** (15%): mp 187 °C; <sup>1</sup>H NMR, DMSO-*d*<sub>6</sub>,  $\delta$  7.1 (d,  $J = 9$  Hz, 1H), 7.40 (m, 1H), 7.56 (m, 2H), 7.82 (m, 1H), 8.0 (d,  $J = 8$  Hz, 1H), 13.84 (s, 1H).

**Biological Methods. In Vitro Aldose Reductase Inhibition Assay.** Test compound (TC) solutions were prepared by dissolving TC in 20  $\mu$ L of 20% dimethyl sulfoxide (DMSO) and diluting with 100 mM potassium phosphate buffer, pH 7.0, to various TC concentrations, typically ranging from 5 mM to 1  $\mu$ M. A "zero TC" solution was prepared that started with only 20  $\mu$ L of DMSO (no TC).

The assay for AR activity was performed in a 96-well plate. Initiation of the reaction (with substrate) was preceded by a 10-min preincubation at 24 °C of 200  $\mu$ L of 100 mM potassium phosphate buffer, pH 7.0, containing 125  $\mu$ M NADPH and 12.5 nM human recombinant aldose reductase (Wako Chemicals, Inc., #547-00581) with 25  $\mu$ L of TC solution. The reaction was initiated by the addition of 25  $\mu$ L of 20 mM D-glyceraldehyde (Sigma, St. Louis, MO). The rate of decrease in OD<sub>340</sub> was monitored for 15 min at 24 °C in a 340 ATTC Plate Reader (SLT Lab Instruments, Austria). Inhibition by TC was measured as the percentage decrease in the rate of NADPH oxidation as compared to a non-TC-containing sample.

**Nerve and Lens Sorbitol Assay in Diabetic Rats:** The acute and chronic tests were done according to the method of Mylari et al.<sup>29a</sup>

**Nerve Fructose Assay in Diabetic Rats: Acute Model.** Male CD Sprague-Dawley rats (175–225 g) were made diabetic by injection of STZ (17 mg/mL in 0.01 M citrate buffer, pH 4.5, 85 mg/kg body wt) into the tail vein of conscious rats. STZ was administered at approximately 9:00 a.m. on day 1. The animals were maintained with free access to food and water. Test compound was administered by oral gavage (volume of 5 mL/kg) at 4, 7, and 24 h after STZ administration. Four hours after the final dose (28 h after STZ administration), animals were sacrificed by cervical dislocation. The left sciatic nerve was excised, weighed, and placed in 1 mL of ice-cold 6% perchloric acid and frozen for fructose analysis at a later date. Weighed sciatic nerves in 6% (w/v) perchloric acid (1 mL) were thawed and homogenized with a Polytron (Kinematica). After the mixture was centrifuged, the decanted supernatant was neutralized by the addition of 3.0 M potassium carbonate (100  $\mu$ L) and recentrifuged. The fructose contents of the supernatants were determined enzymatically.<sup>41</sup> Briefly, fructose was oxidized to 5-keto-fructose by fructose dehydrogenase (FDH) with concomitant reduction of resazurin to the highly fluorescent resorufin. Final assay concentrations were 0.2 M citric acid, pH 4.5, containing 13.2  $\mu$ M resazurin, 1.7 units/mL of FDH, and 0.068% (v/v) Triton X-100. Reaction mixtures were incubated for 60 min at room temperature in a closed drawer. The sample fluorescence was determined at excitation = 560 nm, emission = 580 nm, and slits of 5 mm each (Perkin-Elmer model LS50B fluorescence spectrophotometer). After the appropriate blanks from each sample were subtracted, the nanomoles of fructose in each sample was then determined by comparison with a linear regression of the fructose standards.

**Nerve Fructose Assay in Diabetic Rats: Chronic Model.** Male CD Sprague-Dawley rats (175–225 g) were made diabetic by the injection of STZ (17 mg/mL in 0.01 M citrate buffer, pH 4.5, 85 mg/kg body wt) into the tail vein of conscious rats. STZ was administered at approximately 9:00 a.m. on day 1. The animals were maintained with free access to food and water. On day 8, at 9:00 a.m., test compound was administered by oral gavage (volume of 5 mL/kg). Dosing continued once daily at 9:00 a.m. for 5 days. Four hours after the final dose (day 12), animals were sacrificed by cervical dislocation. The left sciatic nerve was excised, weighed, and placed in ice-cold 6% (w/v) perchloric acid (1 mL) and frozen

for fructose analysis at a later date, using the methods described above.

**Supporting Information Available:** Elemental analysis data. This material is available free of charge via the Internet at <http://pubs.org>.

## References

- (1) (a) Wild, S.; Roglic, G.; Green, A.; Sicree, R.; King, H. Global Prevalence of Diabetes: Estimates for the Year 2000 and Projections for 2030. *Diabetes Care* **2004**, *27*, 1047–1053. (b) Zimmet, P. Z.; Alberti, K. G. M. M.; Shaw, J. Global and Societal Implications of the Diabetes Epidemic. *Nature* **2001**, *414*, 782–787.
- (2) American Diabetes association. Economic Costs of Diabetes in the US in 2002. *Diabetes Care* **2003**, *26*, 917–932.
- (3) The Diabetes Control and Complications Trial Research Group. The Effect of Intensive Treatment of Diabetes on the Development and Progression of Long-term Complications in Insulin-dependent Diabetes Mellitus. *N. Engl. J. Med.* **1993**, *329*, 977–986.
- (4) U. K. Prospective Diabetes Study Group. Intensive Blood-glucose Control with Sulfonylureas or Insulin Compared with Conventional Treatment and Risk of Complications in Patients with Type 2 Diabetes (UKPDS 33). *Lancet* **1998**, *352*, 837–853.
- (5) (a) Hers, H. G. Le Mécanisme de la Transformation de Glucose en Fructose par les Vésicules Seminales. *Biochim. Biophys. Acta* **1956**, *22*, 202–203. (b) Hers, H. G. L'Aldose Reductase. *Biochim. Biophys. Acta* **1960**, *37*, 120–126.
- (6) (a) Van Heyningen, R. Formation of Polyols by Lens of the Rat with "Sugar" Cataract. *Nature* **184**, 194–195, 1959. (b) Gabbay, K. H.; Merola, L. O.; Field, R. A. Sorbitol Pathway: Presence in Nerve and Cord with Substrate Accumulation in Diabetes. *Science* **1966**, *151*, 209–210. (c) Gabbay, K. H. The Sorbitol Pathway and Complications of Diabetes. *N. Engl. J. Med.* **1973**, *194*, 1085–1087. (d) Oates, P. J. The Polyol Pathway and Diabetic Complications. In *The Neurobiology of Diabetic Neuropathy*; Tomlinson, D. R., Ed.; Academic Press: London, 2002; Vol 50, pp 325–392.
- (7) (a) Kinoshita, J. H. A Thirty Year Journey in the Polyol Pathway. *Exp. Eye Res.* **1990**, *50*, 567–573. (b) Kinoshita, J. H.; Nishimura, C. The Involvement of Aldose Reductase in Diabetic Complications. *Diabetes Metab. Rev.* **1988**, *4*, 323–337.
- (8) (a) Tilton, R. G.; Chang, K.; Nyengaard, J. R.; Van den Enden, M.; Ido, Y.; Williamson, J. R. Inhibition of Sorbitol Dehydrogenase. Effects on Vascular and Neural Dysfunction in Streptozotocin-induced Diabetic rats. *Diabetes* **1995**, *44*, 234–242. (b) Williamson, J. R.; Chang, K.; Frangos, M.; Hasan, K. S.; Ido, Y.; Kawamura, T.; Nyengaard, J. R.; Van den Enden, M.; Kilo, C.; Tilton, R. G. Hyperglycemic Pseudohypoxia and Diabetic Complications. *Diabetes* **1993**, *42*, 801–813.
- (9) (a) Geisen, K.; Utz, R.; Grottsch, H.; Lang, J.; Nimmegern, H. Sorbitol-accumulating Pyrimidines: *Arzneim. Forsch. / Drug Res.* **1994**, *44*, 1032–1043. (b) Mylari, B. L.; Oates, P. J.; Beebe, D. A.; Brackett, N. S.; Coutcher, J. B.; Michael S. Dina, M. S.; Zembrowski, W. J. Sorbitol Dehydrogenase Inhibitors (SDIs): A New Potent, Enantiomeric SDI, 4-[2-(1R-Hydroxy-ethyl)-pyrimidin-4-yl]-piperazine-1-sulfonic Acid Dimethylamide. *J. Med. Chem.* **2001**, *44*, 2695–2700.
- (10) Cameron, N. E.; Cotter, M. A.; Basso, M.; Hohman, T. C. Comparison of the Effects of Inhibitors of Aldose Reductase and Sorbitol Dehydrogenase on Neurovascular Function, Nerve Conduction and Tissue Polyol Pathway Metabolites in Streptozotocin-Diabetic Rats. *Diabetologia* **1997**, *40*, 271–281.
- (11) Ao, S.; Shingu, Y.; Kikuchi, C.; Takano, Y.; Nomura, K.; Fujiwara, T.; Ohkubo, Y.; Notsu, Y.; Yamaguchi, I. Characterization of a Novel Aldose Reductase Inhibitor, FR74366, and Its Effects on Diabetic Cataract and Neuropathy in the Rat. *Metabolism* **1991**, *40*, 77–87.
- (12) Egger, J. F.; Larson, E. R.; Lipinski, C. A.; Mylari, B. L.; Urban, F. J. In *Advances in Medicinal Chemistry*; Maryanoff, E., Maryanoff, C. A., Eds.; Jai Press Inc.: London, 1993; Vol. 2, pp 197–246.
- (13) (a) Beyer-Mears, A.; Cruz, E.; Edelist, T.; Varagiannis, E. Diminished Proteinuria in Diabetes Mellitus and Its Prevention by Sorbinil, an Aldose Reductase Inhibitor. *Pharmacology* **1986**, *32*, 52–60. (b) Goldfarb, S.; Simmons, D. A.; Kern, E. F. O. Amelioration of Glomerular Hyperfiltration in Acute Experimental Diabetes Mellitus by Dietary Myo-inositol Supplementation and Aldose Reductase Inhibition. *Trans. Assoc. Am. Physicians* **1986**, *99*, 67–72. (c) Oates, P. J.; Ellery, C. A. Aldose Reductase Inhibitor Zopolrestat Prevents Elevated Urinary Albumin Excretion in Diabetic Rats. *Diabetes* **1992**, *41* (supplement 1), A121. (d) Oates, P. J.; Ellery, C. A. Aldose Reductase Inhibitor Zopolrestat Reduces Hyperfiltration and Albuminuria in Diabetic Rats. *Diabetes* **1992**, *41* (supplement 1), A148. (e)

- Pedersen, M. M.; Christiansen, J. S.; Mogensen, C. E. Reduction of Glomerular Hypertension in Normoalbuminuric IDDM Patients by 6 Months of Aldose Reductase Inhibition. *Diabetes* **1991**, *40*, 527–531.
- (14) (a) Ramasamy, R.; Trueblood, N.; Schaefer, S. Metabolic Effects of Aldose Reductase Inhibition During Low-Flow Ischemia and Reperfusion. *Am. J. Physiol.* **1998**, *275*, H 195–303. (b) Ramasamy, R. Aldose Reductase: A Novel Target for Cardioprotective Effects. *Curr. Drug Targets* **2003**, *4*, 625–632. (c) Kaneko, M.; Ramasamy, R. Aldose Reductase: A Key Player in Myocardial Ischemic Injury. *Exer. Sci. Sport. Rev.* **2004**, *32*, 19–23. (d) Hwang, Y. C.; Kaneko, M.; Bakr, S.; Liao, H.; Lu, Y.; Lewis, E. R.; Yan, S.; Li, S.; Itakura, M.; Rui, L.; Skopicki, H.; Homma, S.; Schmidt, A. M.; Oates, P. J.; Szabolcs, M.; Ramasamy, R. Central Role for Aldose Reductase Pathway in Myocardial Ischemic Injury. *FASEB J.* **2004**, *18*, 1192–1199.
- (15) Ho, E. C. M.; Lam, K. S. L.; Chung, S. S. M.; Chung, S. K. Aldose Reductase Deficient Mice are Alleviated from the Depletion of GSH in the Peripheral Nerve and MNCV Deficit Associated with Diabetes. *Diabetes* **2001**, *50* (Suppl. 2), A59.
- (16) (a) Demaine, A.; Cross, D.; Millward, A. Polymorphism of the Aldose Reductase Gene and Susceptibility to Retinopathy in Type I Diabetes Mellitus. *Invest. Ophthalmol. Vis. Sci.* **2000**, *41*, 4064–4068. (b) Heesom, A. E.; Millward, A.; Demaine, A. G. Susceptibility to Diabetic Neuropathy in Patients with Insulin Dependent Diabetes Mellitus is Associated with a Polymorphism at the 5' end of the Aldose Reductase Gene. *J. Neurol. Neurosurg. Psychiatry* **1998**, *64*, 213–216.
- (17) Negoro, T.; Murata, M.; Ueda, S.; Fujitani, B.; Kuromiya, M.; Suzuki, K.; Matsumoto, J. Novel, Highly Potent aldose Reductase Inhibitors: R-(–)-2-(4-Bromo-2-fluorobenzyl)-1,2,3,4-Tetrahydropyrrolo[1,2-*a*]pyrazine-4-spiro-3'-pyrrolidine-1,2',3,5'-tetrone (AS-3201) and Its Congeners. *J. Med. Chem.* **1998**, *41*, 4118–4129.
- (18) Bril, V.; Buchanan, R. A. Aldose Reductase Inhibition by AS-3201 in Sural Nerve from Patients with Diabetic Sensorimotor Polyneuropathy. *Diabetes Care* **2004**, *27*, 2369–2375.
- (19) (a) Malamas, M. S.; Hohman, T. C.; Millen, J.; Malamas, M. S.; Hohman, T. C.; Millen, J. Novel Spirosuccinimide Aldose Reductase Inhibitors Derived from Isoquinoline-1,3-diones: 2-[(4-Bromo-2-fluorophenyl)methyl]-6-fluorospiro[isoquinoline-4(11*H*),3'-pyrrolidine]-1,2',3,5'(2*H*)-tetrone and Congeners. 1. *J. Med. Chem.* **1994**, *37*, 2043–2058. (b) Hohman, T. C.; Bochenek, W. J.; Meng, X.; Neefe, L.; Beg, M.; Ari, D. T. Nerve Function and Biochemistry in Diabetic Patients Treated with ARI-509, a Novel Aldose Reductase Inhibitor. *Diabetologia* **1997**, *40*, A552.
- (20) Johnson, B. F.; Nesto, R. W.; Pfeifer, R. W.; Slater, W. R.; Vinik, A. I.; Chyun, D. A.; Law, G.; Wackers, F. J.; Young, L. H. Cardiac Abnormalities in Diabetic Patients with Neuropathy: Effects of Aldose Reductase Inhibitor Administration. *Diabetes Care* **2004**, *27*, 448–454.
- (21) Mylari, B. L.; Armento, S. J.; Beebe, D. A.; Conn, E. L.; Coutcher, J. B.; Dina, M. S.; O'Gorman, M. T.; Linhares, M. C.; Martin, W. H.; Oates, P. J.; Tess, D. A.; Withbroe, G. J.; Zembrowski, W. J. A Highly Selective, Non-Hydantoin, Non-Carboxylic Acid Inhibitor of Aldose Reductase with Potent Oral Activity in Diabetic Rat Models: 6-(5-Chloro-3-methylbenzofuran-2-sulfonyl)-2-*H*-pyridazin-3-one. *J. Med. Chem.* **2003**, *46*, 2283–2286.
- (22) Takabayashi, N. Synthesis of Pyridazine Derivatives. VI. Oxidation Products of Sulfur-containing Compounds of Pyridazine. *J. Pharm. Soc. Jpn.* **1956**, *76*, 1293–1296.
- (23) Turck, A.; Ple, N.; Pollet, P.; Queguiner, G. Metallation of tert-Butyl Sulfoxides, Sulfones and Sulfonamides of Pyridazine and Pyrazine. Metallation of Diazines. XX. *J. Heterocycl. Chem.* **1998**, *35*, 429–436.
- (24) Kukulja, S.; Crniac, Z.; Kolbah, D. Nucleophilic Substitution, Demethylation and Methylation in Heterocyclic Series. *Tetrahedron* **1963**, *19*, 1153–1157.
- (25) Mylari, B. L.; Beyer, T. A.; Siegel, T. W. A Highly Specific Aldose Reductase Inhibitor: Ethyl 1-Benzyl-3-hydroxy-2(5*H*)-oxopyrrole-4-carboxylate, and Its Congeners. *J. Med. Chem.* **1991**, *34*, 1011–1018.
- (26) (a) Subatomic and Atomic Crystallographic Studies of Aldose Reductase: Implications for Inhibitor Binding. Podjorny, A.; Cachau, R. E.; Schenider, T.; Van Zadt, M.; Joachiniak, A. *Cell. Mol. Life Sci.* **2004**, *61*, 769–773. (b) Aldose Reductase Structures: Implications for Mechanism and Inhibition. El-Kabbani, O.; Ruiz, F.; Darmanian, C.; Chung, R. P. T. *Cell. Mol. Life Sci.* **2004**, *61*, 750–762.
- (27) Nitta, Y.; Yoneda, F.; Ohtaka, T.; Kato, T. Pyridazinone Derivatives. V. Synthesis of Derivatives of 6-Phenyl-3(2*H*)-Pyridazinone. *Chem Pharm Bull (Tokyo)* **1964**, *12*, 69–73.
- (28) Heinisch, G.; Langer, T. J. Pyridazines. LXVIII. Convenient Synthesis of Phenyl (6-Substituted 3-Pyridazinyl) Ketones via the Oxidative Decyanation Route. *Heterocycl. Chem.* **1993**, *30*, 1685–1690.
- (29) Stribling, D.; Mirrlees, D. J.; Harrison, H. E.; Earl, D. C. Properties of ICI 128, 436, a Novel Aldose Reductase Inhibitor, and Its Effects on Diabetic Complications in the Rat. *Metabolism* **1985**, *34*(4), 336–44.
- (30) (a) Mylari, B. L.; Larson, E. R.; Beyer, T. A.; Zembrowski, W. J.; Aldinger, C. E.; Dee, M. F.; Siegel, T. W.; Singleton, D. H. Novel, Potent Aldose Reductase Inhibitors: 3,4-Dihydro-4-oxo-3-[[5-(trifluoromethyl)-2-benzothiazolyl]methyl]-1-phthalazineacetic Acid (zopolrestat) and Congeners. *J. Med. Chem.* **1991**, *34*, 108–122. (b) Mylari, B. L.; Beyer, T. A.; Scott, P. J.; Aldinger, C. E.; Dee, M. F.; Siegel, T. W.; Zembrowski, W. J. Potent, Orally Active Aldose Reductase Inhibitors Related to Zopolrestat: Surrogates for Benzothiazole Side Chain. *J. Med. Chem.* **1992**, *35*, 457–465.
- (31) Wilson, D. K.; Tarle, I.; Petrash, J. M. Quiocho, F. A. Refined 1.8 Å Structure of Human Aldose Reductase Complexed with the Potent Inhibitor Zopolrestat. *Proc. Natl. Acad. Sci. U.S.A.* **1993**, *90*, 9847–9851.
- (32) Kato, K.; Nakayama, K.; Mizota, M.; Miwa, I.; Okuda, J. Properties of Novel Aldose Reductase Inhibitors, M16209 and M16287, in Comparison with Known Inhibitors. ONO-2235 and Sorbinil. *Chem. Pharm. Bull. (Tokyo)* **1991**, *39*, 540–545.
- (33) Robertson, M. J.; Barnes, J. C.; Drew, G. M.; Clark, K. L.; Marshall, F. H.; Michel, A.; Middlemiss, D.; Ross, B. C.; Scopes, D.; Dowle, M. D. Pharmacological Profile of GR117289 In Vitro: A Novel, Potent and Specific Non-peptide Angiotensin AT1 Receptor Antagonist. *Br. J. Pharmacol.* **1992**, *107*, 1173–1180.
- (34) Jones, J. F.; Mysinger, M.; Korzekwa, K. R. Computational Models for Cytochrome P450: A Predictive Electronic Model for Aromatic Oxidation and Hydrogen Atom Abstraction. *Drug Metab. Dispos.* **2002**, *30*, 7–12.
- (35) Lewis, D. F. V.; Sams, C.; Loizou, G. D. A Quantitative Structure–Activity Relationship Analysis on a Series of Alkyl Benzenes Metabolized by Cytochrome P450 2E1. *J. Biochem. Mol. Toxicol.* **2003**, *17*, 47–52.
- (36) Oates, P. J.; Beebe, D. A.; Coutcher, J. B.; Quian, Y.-Z.; Phillips, D.; Lowe, V.; Appelton, T.; Rauning, D.; O'Neill, S.; Mylari, B. L. Sorbitol Dehydrogenase Inhibition as Well as Aldose Reductase Inhibition Prevents Elevation of Urinary Albumin Excretion in Diabetic Rats. *Diabetologia* **2004**, *47* (Suppl. 1), A398.
- (37) Bosron, W. F.; Prairie, R. L. Triphosphopyridine Nucleotide-linked Aldehyde Reductase. I. Purification and Properties of the Enzyme from Pig Kidney Cortex. *J. Biol. Chem.* **1972**, *247*, 4480–4485.
- (38) Vallee, B.; Hoch, F. Zinc: A Component of Yeast Alcohol Dehydrogenase. *Proc. Natl. Acad. Sci.* **1955**, *41*, 327.
- (39) Siegel, T. W.; Smith, S. R.; Ellery, C. A.; Williamson, J. R.; Oates, P. J. An Enzymatic Fluorimetric Assay for Fructose. *Anal. Biochem.* **2000**, *280*, 329–331.
- (40) Grubenmann, W.; Erlenmeyer, H. Über Bromierte Cumaron-derivate und über eine Neue Darstellung von Cumaronyl-3-essigsäure. *Helv. Chim. Acta* **1948**, *31*, 78.
- (41) Larock, R. C.; Stinn, D. E. Synthesis of Benzofurans Via Palladium-Promoted Cyclization of Ortho-Substituted Aryl Allyl Ethers. *Tetrahedron Lett.* **1988**, *29*, 4687–4690.
- (42) Barnse, R. A.; Gordon, L. Substituted Isobutyrophenones. *J. Am. Chem. Soc.* **1950**, *72*, 5308.
- (43) Chapman, N. B.; Clarke, K.; Iddon, B. Synthesis of Some 5-Substituted Benzo[*b*]thiophenes Related to Gramine. *J. Chem. Soc.* **1965**, 774–777.

JM050462T